FLASH PHOTOLYSIS AND THE RECOMBINATION OF IODINE ATOMS

Thesis by

Don Louis Bunker

In Partial Fulfillment of the Requirements

For the Degree of

Doctor of Philosophy

California Institute of Technology

Pasadena, California

1957

ACKNOWLEDGMENTS

I am very grateful to Professor Norman Davidson, who directed the research described in this thesis, for his encouragement, criticism, and patient guidance.

I would like to thank the General Electric Company for a fellowship (1955-56), the National Science Foundation for two fellowships (1953-55), and the Office of Naval Research for summer support and for a research assistantship (1956-57).

This research was supported by the Office of Naval Research.

ABSTRACT

The rate of recombination of iodine atoms in the presence of argon has been redetermined by a flash photolysis technique. The measured rate constant agrees with results obtained by the same method in other laboratories. The recombination rate has also been measured at temperatures up to 548 ^{o}K; these results are in accord with shock tube data and with other flash photolysis experiments. The rate is found to decrease slowly with increasing temperature, as about $T^{-3/2}$.

In experiments at temperatures between 300 ^{o}K and 493 ^{o}K n-butane has been employed as "third body." It is found to be 13 times more efficient than argon at room temperature; this margin decreases as the temperature is raised. The third-body efficiencies of hydrogen and deuterium have been compared at 323 ^{o}K; they are equal.

The above experiments collectively lead to a determination of the rate of the recombination reaction involving I_2 itself as third body. This reaction is about 600 times more rapid than that occurring with argon at room temperature, but rapidly becomes insignificant if the temperature is increased. From its temperature dependence $\Delta H = -5.32$ Kcal may be deduced for the reaction $I+I_2 \rightleftharpoons I_3$.

TABLE OF CONTENTS

I. INTRODUCTION

This thesis reports the sixth measurement of the rate of the reaction

(1) $$I + I + A \longrightarrow I_2 + A$$

by flash photolysis at room temperature. In addition, a number of measurements have been carried out in which the "third body" required in the homogeneous gas-phase recombination is a species other than argon.

Of the preceding five investigations, three (1,2,3) yielded erroneous and diverging results because the role of molecular iodine as a highly effective third body was not suspected at the time the data were interpreted. In retrospect, the remarkable efficiency of I_2 is not surprising in view of the work of Russell and Simons (2), who compared the third-body effectiveness of 31 gases ranging in efficiency from helium to mesitylene and found a 240-fold variation in the rate constant for the recombination. Christie, Norrish and Porter (4), in studying the cause of the disagreement between the existing measurements of the rate of recombination in the presence of argon, were led to conclude that I_2 as a third body is several hundred times more effective than argon and somewhat more effective than even mesitylene.

The work reported here was undertaken in an effort to obtain accurate rate constants for $I + I + A$ and $I + I + I_2$.

Another objective of the investigation was the study of these reactions at several temperatures, for comparison with high-temperature data obtained in this laboratory using the shock tube (5). Concurrently, investigations of this nature have been carried out by Christie, Harrison, Norrish and Porter (6) and by Willard and co-workers (7); the results of these are now available, and, as will be seen, generally agree with ours.

II. DESCRIPTION OF THE METHOD

Ideally, a kinetic flash photolysis apparatus works by the instantaneous photochemical production of an unstable species in sufficient concentration that its disappearance may be followed by means of a continuously recording photoelectric device. In practice, the upper limit to the rate of reaction which may be measured is fixed by the rapidity with which a xenon flash lamp may be discharged in order to bring about the initial reaction (rather than by the response time of the spectrophotometric instruments). The variety of reactions which may be studied is at present limited by the shortage of species which strongly absorb visible light; ultraviolet techniques have not yet been extensively applied to flash photolysis. The latter limitation restricts kinetic studies to reactions involving colored gases which can be dissociated into colorless radicals (e.g. I_2, Br_2, NO_2) or to systems in which a highly colored species (such as NO_3) may be produced. With the present equipment, in a measure-

ment involving one of the above gases, acceptable kinetic measurements may be obtained under conditions where the half-life of the unstable species is as little as one or two hundred microseconds. The recombination of iodine atoms in an appreciable pressure of added gas is a reaction which admirably fulfills the above conditions for measurability.

The vessel in which the reaction is carried out is shown in figure 1. The cylindrical pyrex cell is 32 cm long and 5 cm in diameter. The side arms and U-tube are nowhere less than 3.2 cm inside diameter. Heating the indicated vertical portion of the side arm to 175°C causes 1 atm of argon to circulate through the cell about 4 times per minute because of a thermal siphon effect. If crystalline iodine is placed in the bottom of the U-tube and the outside of the tube held at constant temperature by immersion in a water bath, a steady concentration of iodine in argon can quickly be obtained by circulation of the argon through the U-tube and cell. However, the final concentration cannot be accurately predicted on the basis of the expected vapor pressure of I_2 at the temperature of the water bath. Apparently, thermal equilibrium is not attained in the U-tube because of the high flow rate of the gas. The top of the cell assembly is connected, through a lightly greased stopcock, to a conventional vacuum line.

The cell is enclosed in a cylindrical furnace of 6 inch inside diameter. The furnace consists of an 18 inch

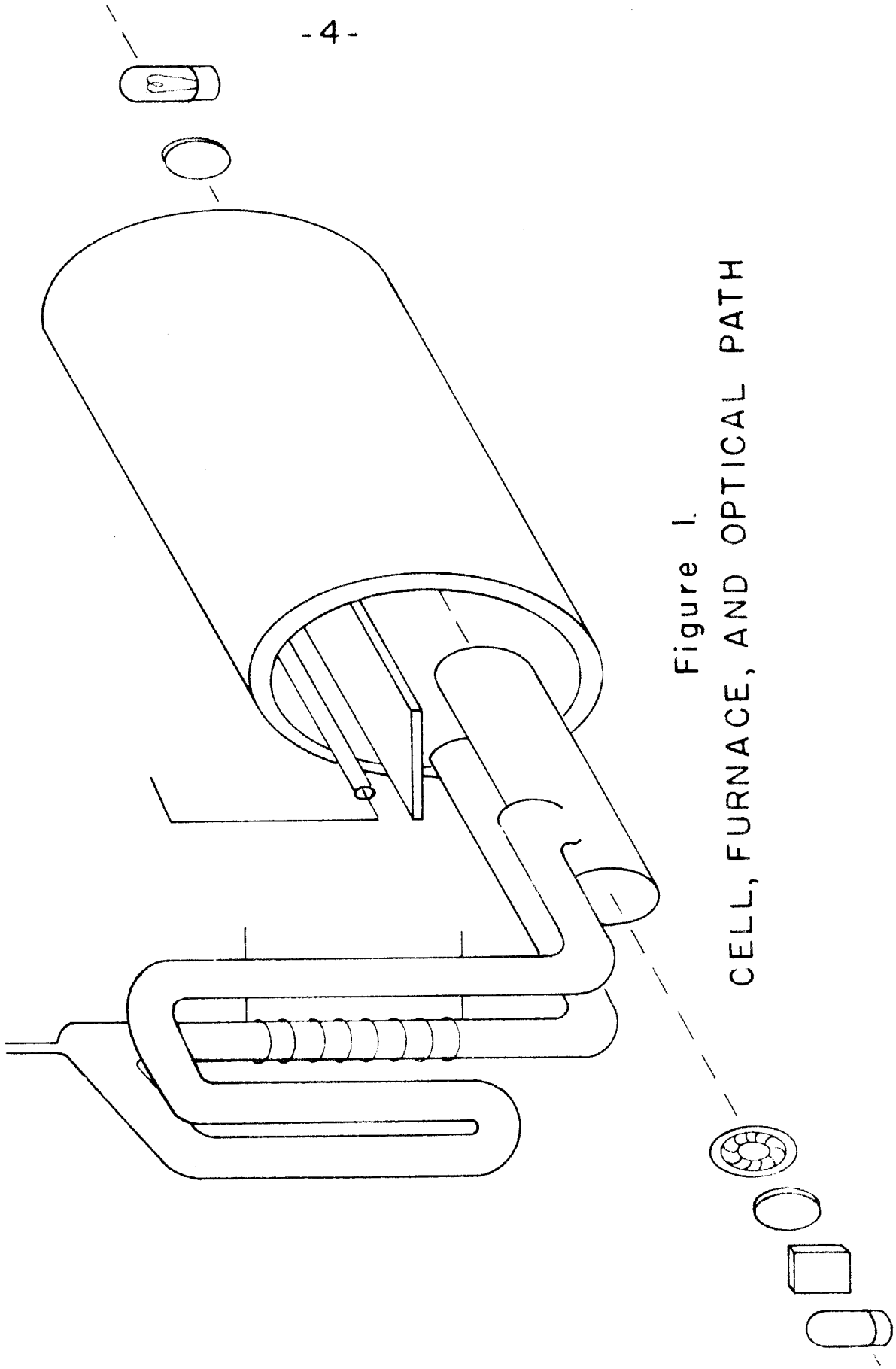

Figure 1.
CELL, FURNACE, AND OPTICAL PATH

length of aluminum pipe covered with asbestos tape and wound with 70 ft of 16 gauge Chromel A wire. The windings, which are closer together at the ends of the furnace for more uniform temperature inside, are covered with magnesia pipe lagging about 2 inches thick. The furnace end plates are of transite, insulated with 2 inches of pyrex wool.

The furnace is mounted horizontally and is divided into two compartments by a layer of Corning No. 3486 glass color filters. The cell is supported in the lower compartment by brackets attached to the bottom of the furnace. The flash lamp is mounted in the upper compartment. The filters and flash lamp are supported from the transite end plates.

The flash lamp is constructed of 13 mm pyrex tubing and is 36 cm long. Electrode leads are of 1 mm tungsten rod; their exterior portion is usually silver soldered to a length of heavy copper bus bar in order to minimize breakage due to the flexing of the tungsten when the lamp is discharged. Electrical connections are made to the bus bar. The lamps are outgassed and filled to 5 cm pressure with xenon.

Various electrode designs have been tried in an effort to achieve long-term reliability. Current practice calls for a cylindrical nickel electrode of about 1/4 inch diameter, with the emissive surface machined to a round or conical shape. These electrodes have a 1 mm hole drilled in their base, into which the tungsten rod is shrink-fitted.

Lamps constructed in this way have exhibited an average life of at least several hundred firings, and fail by breakage or leakage rather than by detachment of the electrodes from their leads.

The temperature of the furnace is controlled by conventional Brown Instrument Company equipment, operating from a chromel-alumel thermocouple inserted through one of the end plates. The temperature along the length of the cell was found to be uniform within 4°C at 250°C. The temperature of the winding on the cell side arm (4 feet of 26 gauge Nichrome) is controlled by a variable transformer and measured by a Leeds and Northrup potentiometer connected to a chromel-alumel thermocouple imbedded in the asbestos insulation covering the winding.

Figure 2 is a block diagram of the measuring and lamp firing circuits. The source of power for the flash lamp is a Condenser Products Company PS-30 30 KV power supply, whose maximum output current is 1 milliampere. The output voltage of this power supply is controlled by a variable transformer across the input. The power supply is used to charge a bank of 4 parallel 1 μF condensers rated for 20 KV. The condensers are in series with the flash lamp and a 5C22 hydrogen thyratron which functions as an on-off switch. This circuit has been described previously (8). In order to reduce the disturbances induced in the measuring circuits by the operation of the flash lamp, the conductor between the condensers-5C22 and the flash lamp is composed

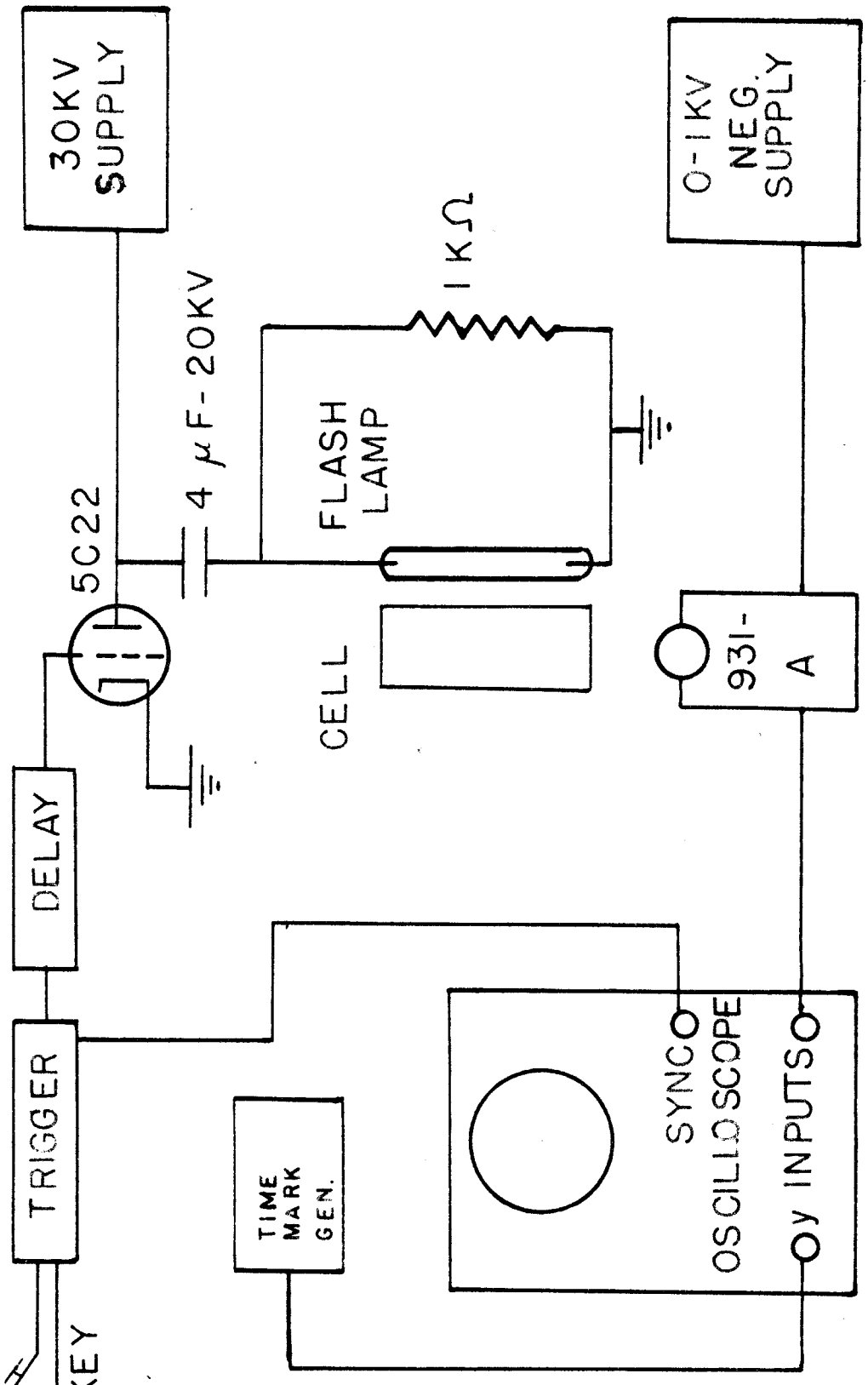

Figure 2. BLOCK DIAGRAM OF APPARATUS

of four coaxial cables bound in a square configuration, with the high voltage leads at opposite corners. Each part of the high-voltage circuit is independently grounded to the cathode of the 5C22, as is the galvanized iron enclosure.

The light source employed in measuring I_2 concentration is a 500 watt tungsten projection lamp operated at 120 volts from storage batteries. The light passes through a condensing lens before entering the reaction cell. Beyond the cell a lens of 10 inch focal length is employed to image the lamp filament on the cathode of a 931-A photomultiplier tube. A 486 mμ interference filter and a Corning No. 3387 yellow filter are interposed between the lens and photomultiplier tube. The filters must be perpendicular to the light path within about 5°. Light intensity is controlled by an iris diaphragm in front of the converging lens.

The multiplying voltage for the photomultiplier tube is obtained from a regulated power supply which furnishes about 50 volts per stage (variable). Ripple and drift are held to a few hundredths of a per cent. For reasons to be discussed, a separate source of collecting voltage is desirable, and a 90-volt battery is used. The photomultiplier circuit also includes a 45-volt battery and precision potentiometer arranged in a bucking circuit so that the DC output signal level may be set at 0 volts, and the actual DC level accurately measured. To facilitate the latter the output is provided with a shorting switch. This equipment

is shown in detail in figure 3. The output of the photomultiplier circuit is connected to the y input of a DuMont 304-H oscilloscope, operating in the DC single sweep mode. Trace photography is done with a DuMont Polaroid type camera.

Proper sequencing of the operation of the instruments includes synchronizing each oscilloscope trace to local 60 cycle alternating current, to provide a means of circumventing the occasional noise component caused by the operation of electric machinery elsewhere in the building. To accomplish this, the power line is monitered through an isolation transformer and a circuit which clips and differentiates the 60 cycle wave form. The first negative pulse obtained from this network, after the key is depressed, is used to trigger an irreversible flip-flop circuit which thereupon generates the 12-volt step function used to initiate the experiment. The 12-volt signal is differentiated to provide a 12-volt spike which starts the oscilloscope single sweep. It is also fed directly into a variable RC delay circuit, including a 2D21 thyraton which discharges a capacitor after the selected delay. The 200-volt positive signal resulting from this discharge is applied to the grid of the 5C22 thyratron, resulting in the connection of the charged 20 KV capacitors to the flash lamp. The delay circuit has also been described previously (9).

Time base calibration is accomplished with a Tektronix type 181 time mark generator. The output of this is inte-

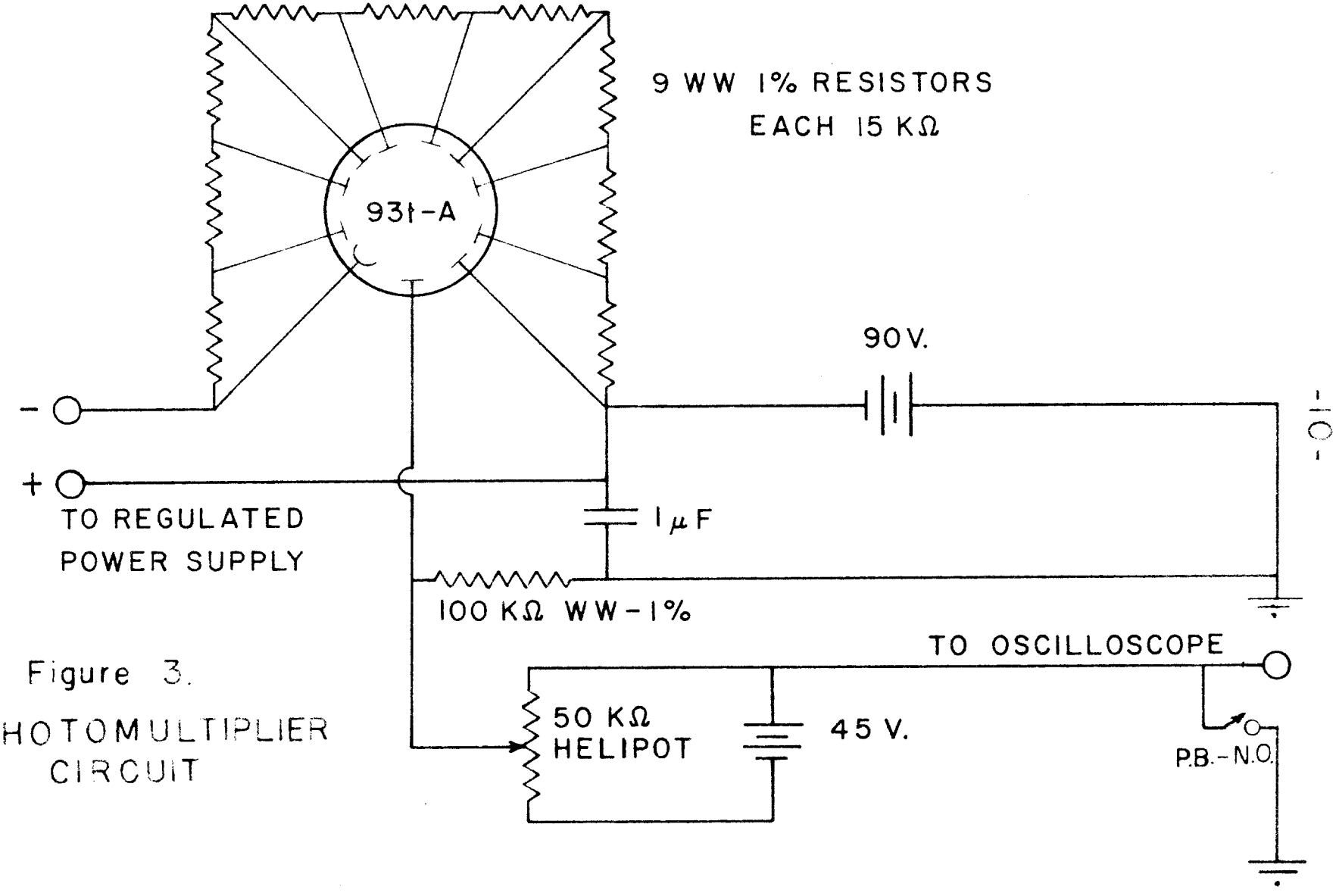

Figure 3.

PHOTOMULTIPLIER
CIRCUIT

grated (for easier photography) and simply photographed with the oscilloscope sweep controls set at the same values as used in the experiment. Experience has shown that if the DuMont oscilloscope is powered from a constant-voltage transformer, the gain and time base are essentially constant after warm-up, and zero drift is greatly reduced.

In an experiment, the instruments and light source are allowed to warm up for at least an hour, in order to attain stability and in particular to fatigue the photomultiplier tube to a point where further change in sensitivity is slow. The chosen pressure of added gas is admitted to the cell. The U-tube, which contains resublimed I_2, is warmed to a temperature corresponding approximately to the pressure of I_2 desired. The gases are then mixed to constant optical density by heating the arm of the thermal siphon. When a steady state is attained, the output of the photomultiplier is adjusted to match the DC zero of the oscilloscope. Photographs (usually seven) are then taken of oscilloscope traces during actual flash photolysis experiments. A photograph is taken of the sweep without the flash lamp discharge, to detect AC noise and possible errors in the alignment of the cathode ray tube. The gases are then pumped from the cell, and the DC signal before and after doing so recorded for use in computing the actual I_2 concentration. Following this, photographs of the flash lamp operating with an empty cell are obtained, to determine the time at which scattered light from the flash lamp

becomes negligible. The time base is photographed. The conversion factor between Helipot units and inches oscilloscope deflection is determined before and after the experiment; the two determinations seldom differ by more than 2 per cent. The furnace temperature may be taken from the Brown controller with sufficient accuracy for the calculation of gas concentrations.

At a particular temperature between 5 and 20 samples of gas are examined in this way. Gas pressures are chosen to cover the range of $[I_2]/[\text{added gas}]$ between the lower limit of excessively fast recombination and the upper limit caused by the onset of the thermal errors discussed in the next section.

III. PERFORMANCE, ERRORS, AND CALCULATION OF RESULTS

1. Data Reduction and Indeterminate Errors

The third order rate constant to be determined will be denoted by k(M, T), where M represents the third body and T the temperature; in case of possible ambiguity it is labelled ^{o}C or ^{o}K. It is defined by

$$(2) \qquad d[I_2]/dt = k(M,T)\,[I]^2\,[M]$$

$$(1/[I]_t) - (1/[I]_o) = 2k(M,T)[M](t - t_o).$$

Units are universally moles per liter and seconds. In terms of the cell length L and decadic extinction coefficient ϵ, the concentrations of I and I_2 are

$$(3) \qquad [I]_t = (2/\epsilon L)\log_{10}(y_t/y_o);$$

$$[I_2]_\infty = (1/\epsilon L)\log_{10}(a/y_o).$$

The oscilloscope deflections are denoted by a = amplitude with cell empty; y_o = amplitude with cell filled, and y_t = $y_o + \Delta y_t$, the amplitude at time t during the experiment. (Time zero is an arbitrary point selected by examination of the discharge time of the flash lamp; the "actual" initial concentration of I atoms can be found by extrapolation. Usually about 10 per cent of the I_2 is dissociated by the flash.) Deflection units can be either inches or Helipot units in the calculation.

Figure 4 shows typical pictures obtained in an experiment. After the flash, the distance from the base line to the trace is Δy_t. This quantity is measured at ten or more points and converted according to equation 3 into $1/[I]_t$, which is plotted against time. The slope of this plot, or its initial slope in cases where a slight (explainable) curvature exists, is determined by eye and equated to $2[M]k(M,T)$; $k(M,T)$ is obtained from this. A representative kinetic plot is shown in figure 5.

The rate constants determined for an individual sample of gas usually spread over a range of about 5 or 10 per cent. The collection of average rate constants for all the gas samples at a given temperature, when plotted against $[I_2]/[M]$ (with $[I_2]$ corrected for extent of dissociation

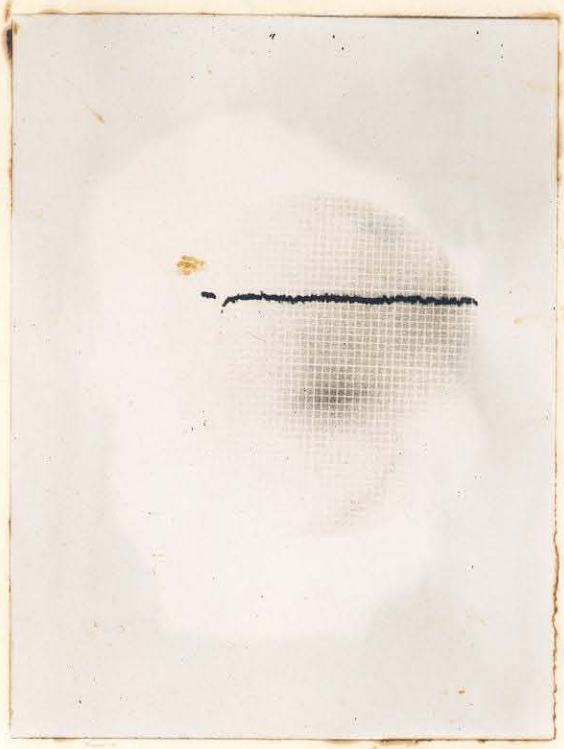

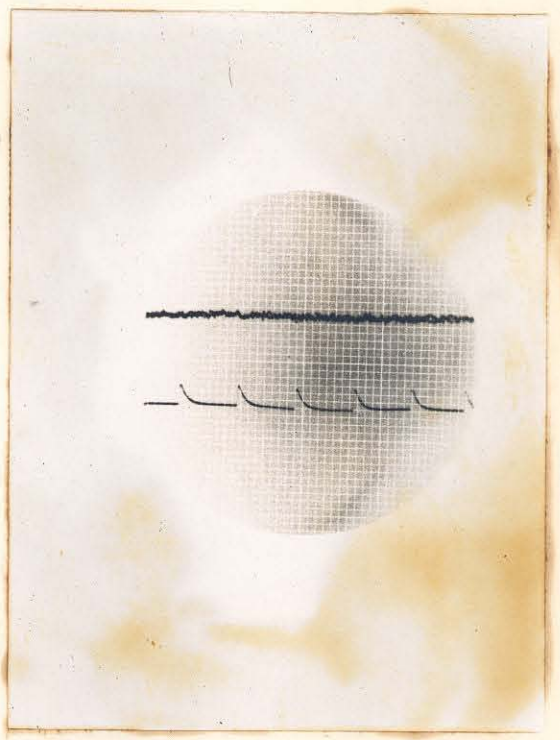

Figure 4. Typical Pictures

(Above) Flash alone; (Upper right) Experiment; (Right) Sweep alone and time base

Upward deflection represents decreasing photocurrent.

Figure 5.
KINETIC PLOT

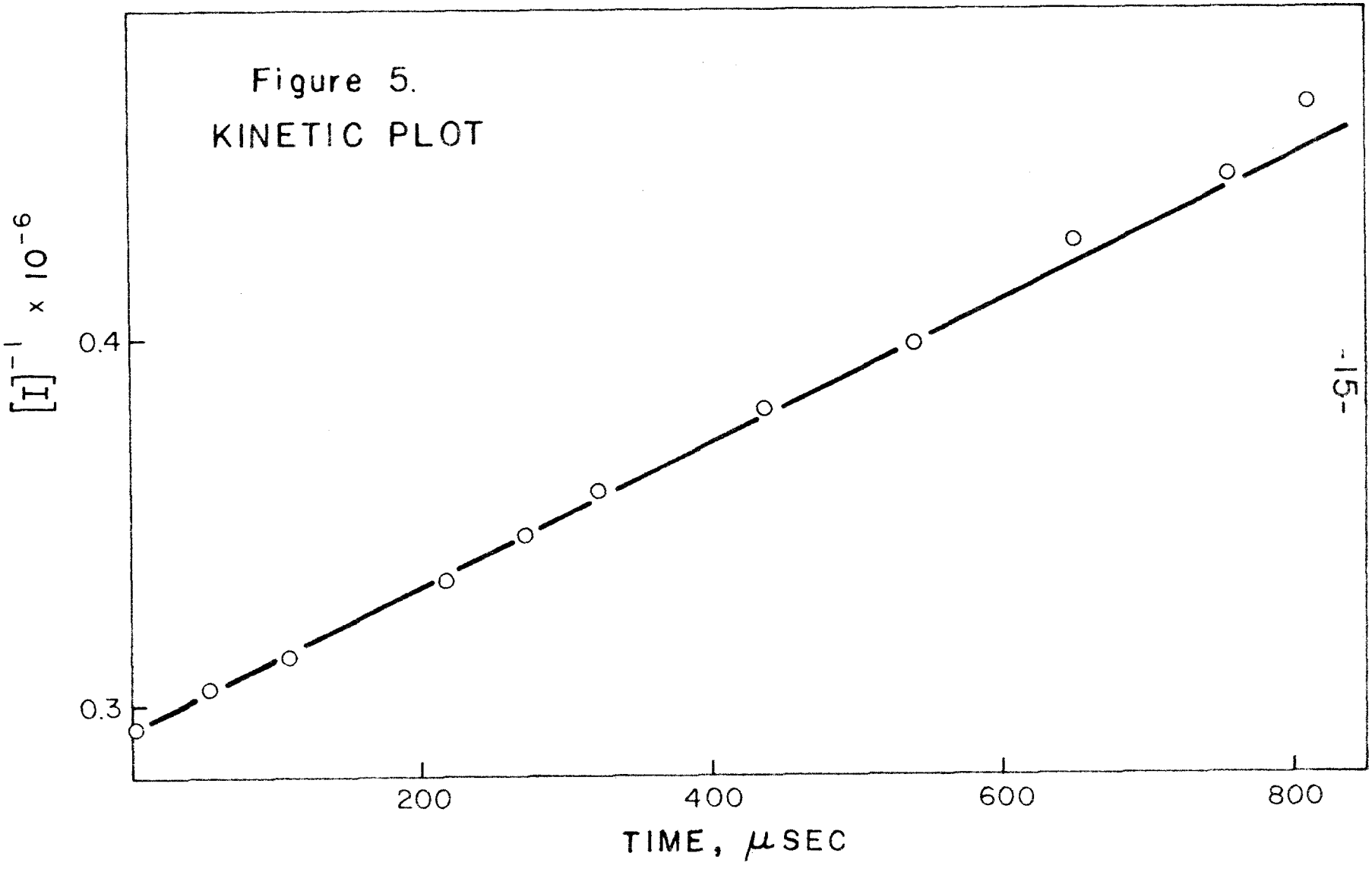

at time zero), forms a good straight line. The slope and intercept of this line are determined by least squares. The intercept gives the final value of $k(M,T)$ at that temperature, and the slope is equivalent to $k(I_2,T)$. Thus every measurement involving an added gas automatically provides an additional measurement of $k(I_2,T)$, and the plots of $k(M,T)$ vs $[I_2]/M$ should have the same slope for different gases as M at the same temperature.

The smallest change in deflection measureable by eye is about .01 inch; both this and the time base stability are more than adequate for a 1 or 2 per cent measurement. The largest indeterminate error in a quantity entering into the calculations is in the scale factor between oscilloscope deflection and Helipot units, which can be determined only to within a few per cent. This, however, contributes to the scatter of the average rate constants rather than to differences between pictures. The rate constants for a given gas sample are scattered by differences in the initial degree of dissociation (resulting in small differences in systematic errors to be discussed) and by noise.

With the photomultiplier tube operated at a gain of approximately 1500, 0.05 microampere of primary photocurrent is ample for the purposes of the experiment (0.5 is commonly obtained). The rise time of the amplifier is about 5 microseconds, the most important factor being the oscilloscope input capacitance. From these two pieces of information

one computes the theoretical signal-to-shot noise ratio, $(it_r/e)^{\frac{1}{2}}$ where e is the electronic charge. Numbers approaching 1000 are obtained, and this corresponds to what is observed. Occasionally extraneous signals of an aperiodic character (commonly caused by mechanical vibration of the optical equipment) are present, and the signal-to-noise ratio is appreciably reduced. Near the end of an experiment $y_o/\Delta y_t$ may be as large as 100, so that in some cases the kinetic plot may become very inaccurate. This circumstance limits the number of half-lives of I atoms during which the concentration may be followed. In a large-signal experiment conducted under conditions of minimum electrical and mechanical interference from the building, it was found possible to extend the experiment to 5 or 6 half-lives before noise caused a deviation from third-order kinetics, provided that correction was made for the effect of the small change in $[I_2]$ on the contribution of $I + I + I_2$ to the recombination. In most experiments, however, only about 1 half-life was followed, in order to minimize thermal effects which, in the test experiment, were depressed by using a very large amount of added gas.

The observed kinetics were also found to be invariant to limited changes in total pressure (i.e. about a factor of 2, governed by the useful range of I_2 vapor pressure), and to the initial degree of dissociation. The latter was varied by changing the storage capacitance from 4 μF to 1 μF.

Errors due to oscilloscope nonlinearity were virtually eliminated by installation of a flat-face cathode ray tube in the oscilloscope, and by frequent adjustment of the horizontal and vertical linearity controls. An area varying between 1/2 and 1 inch wide around the periphery of the tube face always requires linearity correction; no measurements have been made in this area.

The voltage available for operation of the tungsten lamp varied over a 6 volt range with the state of charge of the storage batteries. In connection with the determination of the extinction coefficients (q.v.) the calculation of ϵ was repeated for a light source at a color temperature corresponding to a 10 volt drop in operating voltage, and no change in ϵ was found.

In high-pressure experiments, the recovery time of the instruments is important in determining the reliability of the kinetic measurement. It is not certain whether scattered light or instrumental pickup is more important in establishing the shape of the apparent decay curve of the flash lamp. Scattered light is minimized by judicious choice of filters (cf. section IV on spectrophotometry) and by suitable baffles and enclosures around the optical path. Instrumental noise resulting from the discharge of the flash lamp is difficult to combat; the best measures are physical separation of the measuring and lamp firing circuits, elimination of circular electrical paths through the instrument ground connections, and lavish use of

shielding. The photomultiplier tube has three concentric shields, made of iron, aluminum and iron. With these precautions, the best recovery time (time for signal to become comparable with shot noise) yet obtained is about 200 μsec.

No test for possible non-uniform illumination by the flash lamp was made in this investigation. Flash lamps of the type described here have been previously (1,6,7) shown to radiate approximately the same light intensity from every point on their longer dimension. Since the optical density of the cell and its contents, viewed from the side, is small, most of the flash light passes through the cell again and again before absorption. If, in spite of this, there is an initially non-uniform distribution of I atoms, its effect on the measured rate constant would be expected to be small (7).

2. Photomultiplier Tube Calibration and Correction.

Of the two major systematic errors arising in this experiment, the one most easily remedied is connected with the inherently non-linear response of the 931-A multiplier tube.

A photomultiplier tube is usually thought to possess, within limits, a linear relationship between illumination and amplified photocurrent (10), providing the amplified current is not so large as to saturate the final stages (in this case it is not). This property is universally established with the use of National Bureau of Standards neutral density filters. A somewhat more rigorous test has

been devised in this laboratory in order to measure what might be termed the "differential sensitivity" of the tube. A weak AC light signal, obtained from a glow lamp or by mechanically chopping a DC light beam, is focussed as a spot on the photocathode. A strong DC light signal of variable magnitude is brought to a focus and superimposed on the spot illuminated by the alternating light source. A half-silvered mirror is used to mix the light beams. If the DC source is turned on and off and the variation of the amplitude of the AC signal on the oscilloscope screen noted, the relative differential sensitivity $(dV/dI)_V/(dV/dI)_o$ can be recorded. Here V is output signal and I is light intensity. Since the sensitivity as measured with the filters is $\frac{1}{I}\int_o^I (dV/dI)_V dI$, it is evident that considerable variation in the differential gain could be hidden in the conventional linearity curve; and, in fact, the integral of the sensitivity measured here is consistent with the data given by RCA.

A number of curves representing the relative differential sensitivity as a function of output signal (developed across a 100 KΩ load resistor), for various modes of operation of the tube, are shown in figure 6. It should be noted that if the usual method of power supply is employed, i.e. a single regulated voltage impressed across ten identical dividing resistors between the photocathode and last anode, the response of the tube should be as illustrated by curve C in figure 6 rather than flat. This is because the voltage

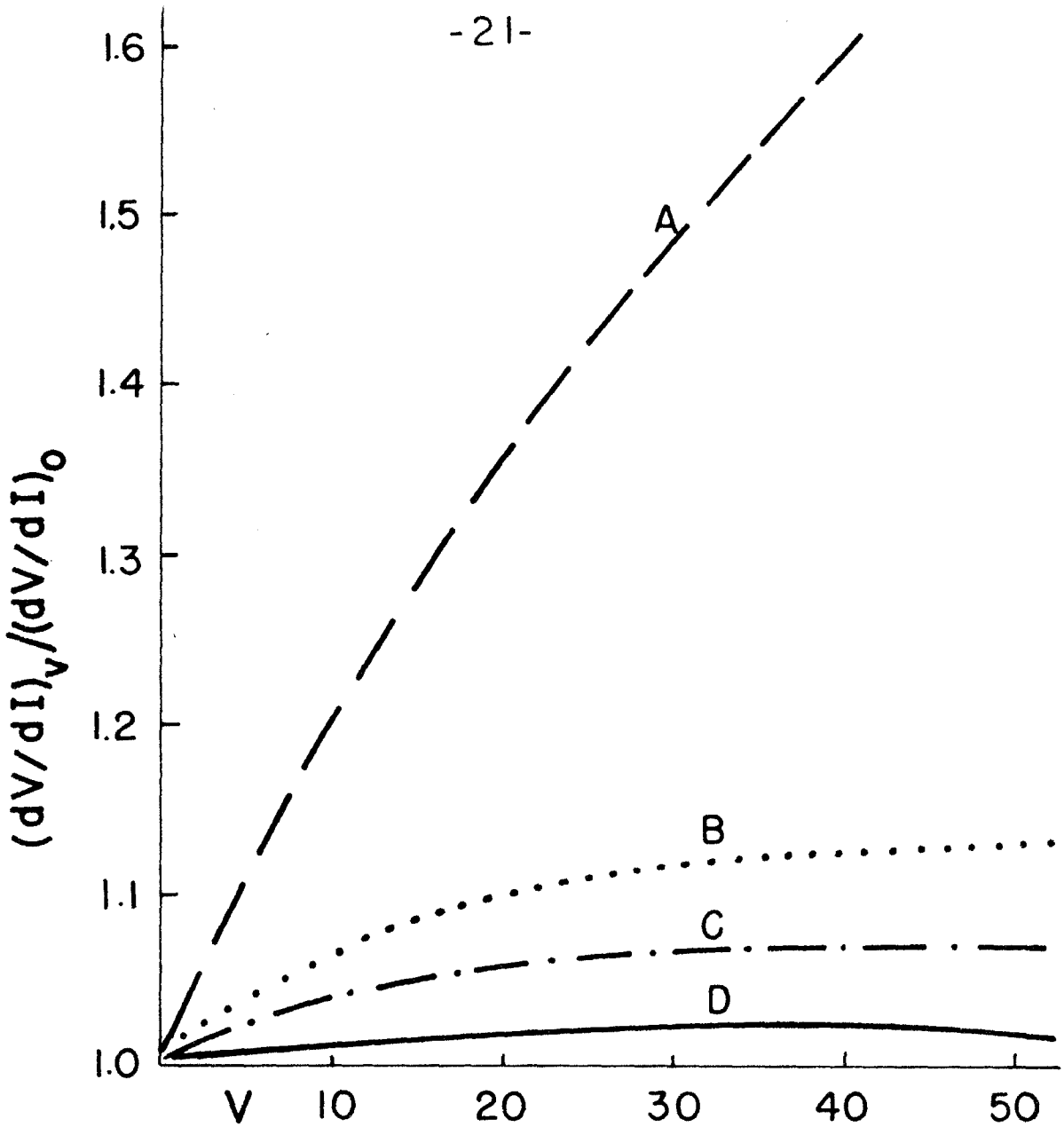

Figure 6.

RELATIVE DIFFERENTIAL SENSITIVITY versus OUTPUT VOLTAGE

A – – – 6 stages
B ..... 10 stages
C —·— Calculated relation
D ——— 10 stages, separate collector

$R_L = 100\ k\Omega$

across the final or collecting stage, in which no amplification occurs, is diminished when an appreciable amplified photocurrent flows. The regulation of the power supply then requires that the voltage across the earlier stages increase in order to maintain a constant total value. Frequently this increase is suppressed by placing a large capacitor across each dividing resistor, but this method cannot be used here because it would tend to delay recovery of the circuit from the pulse of scattered light due to the flash lamp. In any case this method fails if it is necessary to compare two DC signal levels, and this must be done in this experiment in order to determine I_2 concentration. The voltage increase in the earlier stages is reflected in an increase in gain, whose magnitude may be calculated as follows.

In the early experiments only six of the ten dynodes were used; let the gain of each stage be g and the primary photocurrent I_P. The dynodes, resistances and divider currents are labelled as shown in figure 7. If g is the same for every stage and does not change appreciably with the amplified photocurrent at that stage, the current relations are

$$(4) \qquad \begin{aligned} i_{01} + I_P &= i_{12} + gI_P \\ &= i_{23} + g^2 I_P \\ &= i_{34} + g^3 I_P \\ &= i_{45} + g^4 I_P \\ &= i_{56} + g^5 I_P \end{aligned}$$

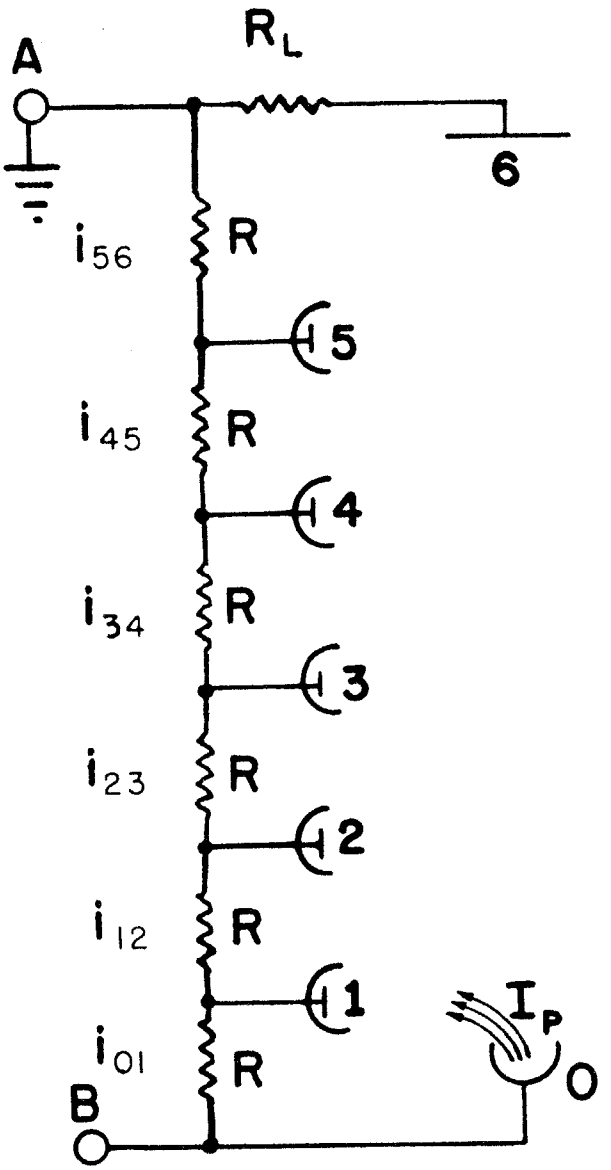

Figure 7.

FIVE-STAGE PHOTOMULTIPLIER CIRCUIT

In addition,

$$(5) \qquad V_{AB} = \text{constant} = R \sum_{s=0}^{5} i_{s,\, s+1}$$

Equations 4 and 5 can be easily solved for the unknown currents, which when multiplied by R give the voltage changes across the dividing resistors. For $I_P = 0.5$ μamp, $R = 25K\Omega$, $V_{AB} = 600$, and $g = 4$,

$$(6) \qquad \Delta V_{01} = \Delta V_{12} = +2.8 \qquad \Delta V_{34} = +2.0$$
$$\Delta V_{23} = +2.6 \qquad \Delta V_{45} = -0.4$$

$$\Delta V_{s,s+1} = I_P R \left[\frac{g^6 - 1}{6(g-1)} - g^s \right] .$$

It can be determined empirically from the gain vs supply voltage characteristic of the tube (10) that, approximately,

$$(8) \qquad \delta_{g/g} = 0.74\, \delta V/V$$

The computed overall gain, nominally $4^5 = 1024 \equiv G$, is for this case

$$(9) \qquad \prod \left(1 + \frac{\delta g}{g}\right) = 1102 \equiv G + \Delta G; \quad \frac{\Delta G}{G} = +.075$$

A set of similar though less compact calculations for a 9-stage multiplier leads to the curve C shown in figure 6. Initially the 5-stage multiplier was selected in order to keep the potential increase between dynodes as large as possible, to minimize defocussing by stray fields radiated

from the flash lamp. This was an unfortunate error because not only does no significant improvement appear in the instrument recovery time, but also the differential sensitivity behaves in the wild fashion shown as curve A. The reason for this is far from clear, but as the sixth dynode in a 931-A bears faint resemblance to a collector anode, some kind of anomalous behavior is certainly to be expected. The situation is vastly improved if the circuit is assembled in the correct way, i.e. using the first 9 dynodes as dynodes and the last as collector; curve B is then obtained. The increase in gain is approximately twice that calculated. No explanation of this phenomenon is forthcoming either. Curve D is obtained by employing a separate battery to collect the amplified photocurrent, thus rendering the sensitivity curve essentially flat. About half the data were obtained under Curve D conditions.

There remains the problem of what to do with the data taken with the 5-stage photomultiplier. Fortunately, computation of a correction factor involves integration of curve A, which makes the discrepancy rather smaller, and the correction to a ratio of two observed deflections is smaller still. Since all the early experiments were done under similar conditions of gain and output signal, it was found possible to make a blanket correction to the final calculated rate constants with only a small sacrifice of claimable accuracy.

To find the correction factor to reduce Helipot readings or inches deflection to what would have been obtained if the sensitivity were everywhere $(dV/dI)_o$, the inverse of curve A, figure 6 is integrated up to the observed output level. That is,

$$(10) \qquad \frac{V_{actual}}{V_{observed}} = \frac{\int_0^V (dI/dV)_V dV}{V_{observed}} = \text{correction factor } x,$$

if $(dV/dI)_o$ is defined as 1. The inverse sensitivity curve and its integral are shown in figure 8.

In the measurement of $[I_2]$, the correction takes the form

$$(11) \qquad [I_2]calc = (1/\epsilon L)\log_{10}(y_2/y_1)$$
$$[I_2]actual = (1/\epsilon L)\log_{10}(x_2y_2/x_1y_1)$$
$$\text{additive correction} = (1/\epsilon L)\log_{10}(x_2/x_1)$$

The range of y_1 was 200-400 (Helipot units) and that of y_2 400-800. The ratio was always near 2. The average decrease in $[I_2]$ required under these conditions is 17 per cent. Use of this figure at the extremes of the range of the y's produces an estimated error of 3 to 6 per cent in $[I_2]$.

The nonlinearity also affects the observed rate constant. In this case we have

$$(12) \qquad [I]_{calc} = (2/\epsilon L)\log_{10} \frac{y + \Delta y}{y} .$$

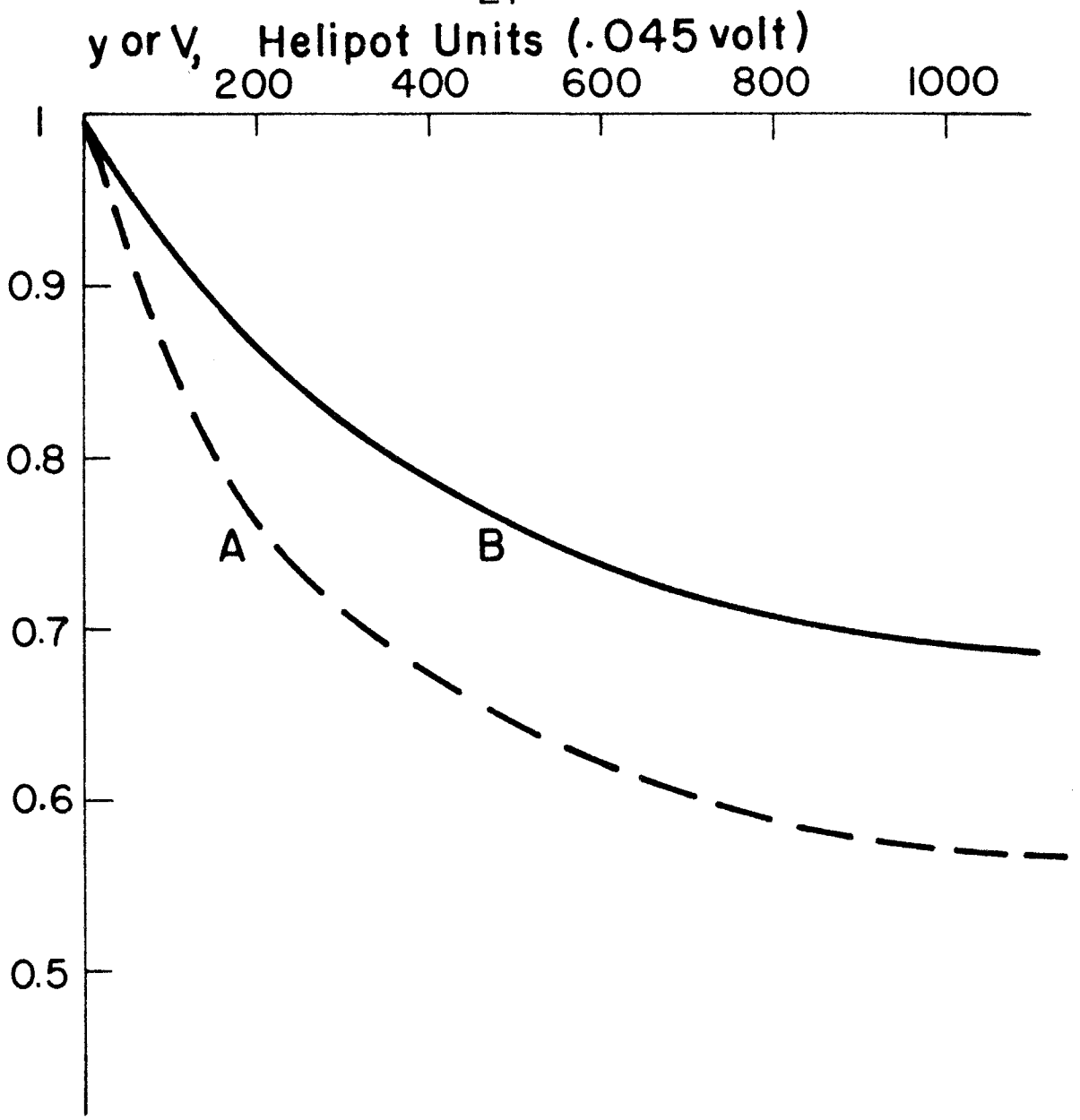

Figure 8.

PHOTOMULTIPLIER CORRECTIONS

A – – – $(dI/dV)_V$

B ——— Correction factor, x

The correction to y is x; to $y+\Delta y$, $x+(dx/dy)_y \Delta y \equiv x - s\Delta y$. The range of y was about 250-450; during the experiment x ran from about .83 to .77 in a typical case, and sometimes reached .93 or .70; s is in the neighborhood of .0003 $\pm$ .00005. The additive correction to [I] is

$$(13) \quad (2/\epsilon L)\log_{10}\frac{x-s\Delta y}{x} = (2/2.303\,\epsilon L)\ln(1-s\Delta y/x)$$

$$= \frac{2}{2.303\epsilon L}\cdot\frac{-s\Delta y}{x}\ , \text{ very closely.}$$

To find a correct expression for 1/[I], one inverts the expression for [I] and expands the resulting denominator, retaining the second term.

$$(14) \quad [I]_{actual} = [I]_{calc} + \frac{2}{2.303\epsilon L}\cdot\frac{-s\Delta y}{x}$$

$$[I]^{-1}_{actual} = [I]^{-1}_{calc} + \frac{2s\Delta y}{2.303\,\epsilon\, Lx} \quad .$$

But since, in expanded form, equation 12 can be rewritten

$$(15) \quad 2\Delta y/2.303\,\epsilon\, L = y/[I]_{calc} \ ,$$

equation 14 is equivalent to

$$(16) \quad [I]^{-1}_{actual} = [I]^{-1}_{calc}\,(1+sy/x).$$

Insertion of the numbers given above reveals that the observed rate constants should be increased by about 13 per cent, and that only a 2 to 4 per cent error will be intro-

duced into the rate constant measurements for which x or s were not typical.

If the effect of these two corrections on the plot of k(M,T) vs $[I_2]/[M]$ is examined, it is found that both corrections apply to the slope, but that only the second affects the intercept. Therefore all the rate constants determined with the 5-stage photomultiplier, of the form k(M,T) where $M \neq I_2$, were multiplied by 1.13 and the probable error widened by 4 per cent of the rate constant; and all the rate constants $k(I_2,T)$ determined in this way were multiplied by 1.13 x 1.17 = 1.32 and their probable error increased by 7 per cent. The corrected rate constants at various temperatures fit smoothly onto the rate constants which did not require correction, and the increased uncertainties are not very detrimental.

3. The Thermal Effect

Optimization of the performance of a flash photolysis apparatus requires the striking of a compromise between various kinds of design, each with advantages and drawbacks. Since (in this investigation) the concentration of the unstable species is determined by measuring small changes in the concentration of the substrate, the measurements are exceedingly sensitive to extraneous fluctuations of the optical density of the stable species. One way to minimize such fluctuations is to increase the range of variation of the optical density, as by increasing the concentration of

(in this case) I_2, or, more easily, increasing the initial degree of dissociation. On the other hand, extensive application of these measures results in more energy being added to the gas sample; this appears as translational energy as the recombination proceeds, and the temperature rise of the gas in the cell may become large. Since recombination proceeds at a rate comparable with heat diffusion, such a temperature rise will be spatially non-uniform and the center of the cell will become warmer than the edges. This can lead to large errors in [I] due to the resulting inhomogeneity in $[I_2]$.

Of the three groups currently making recombination measurements on I atoms (6,7), this laboratory maintains the most nearly isothermal experimental conditions. Our degree of dissociation and total added heat capacity are such that the temperature rise is never more than a few degrees during the entire experiment. At the other end of the scale, Porter and co-workers (3,4,6) employ low pressures, extensive initial dissociation and long flash durations and find that thermal effects are so severe as to require explicit correction. An analysis of the thermal effect is given below. It shows that, under the conditions of our experiments, there are no systematic errors due to heating of the gas, and no corrections are needed. Unfortunately, the analysis which we have developed tends to cast doubt on some of the results of Christie, Harrison, Norrish and Porter (6), hereafter referred to as CHNP.

Since the CHNP model is in some ways a special instance of ours, our calculation is presented first. In our case it is assumed that all the heat appears at the time of the flash, resulting in a temperature rise ΔT. This means that the calculation yields a pessimistic estimate in the early stages of the reaction. CHNP allow ΔT to build up during the course of the reaction; our treatment may be adjusted later to include this, if necessary.

Consider a cylindrical cell of radius r. Immediately after the flash its interior is at $T+\Delta T$ and its boundaries at T, the ambient temperature. At some later time t the mean distance from the boundary into the cell which will have cooled significantly will be given by $\delta r = g\sqrt{Dt}$ where g is a small number between 1 and 3. D is the heat diffusivity, $\lambda/\rho C_v$, and is of the same order of magnitude as the ordinary diffusion coefficient. In our case δr is always less than 0.3 cm so that $\delta r \ll r$.

Figure 9a indicates the temperature profile used to approximate the above condition. The fractional volume which has cooled to T is given by

$$(17) \qquad \frac{V_o}{V} = \frac{2\delta r}{r} \quad (\text{since } \delta r \text{ is small});$$

$$= 2g\sqrt{Dt}/r.$$

With subscripts c referring to the center portion of the cell and o to the outside, the concentration distribution is

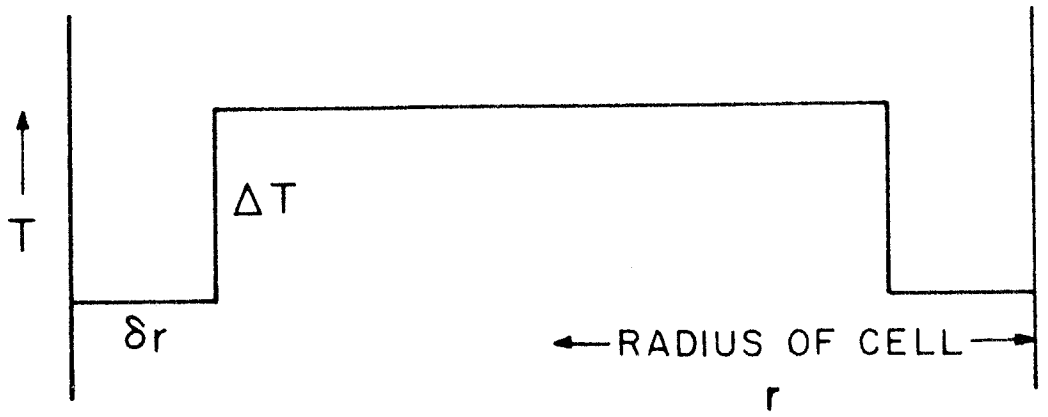

a. This thesis

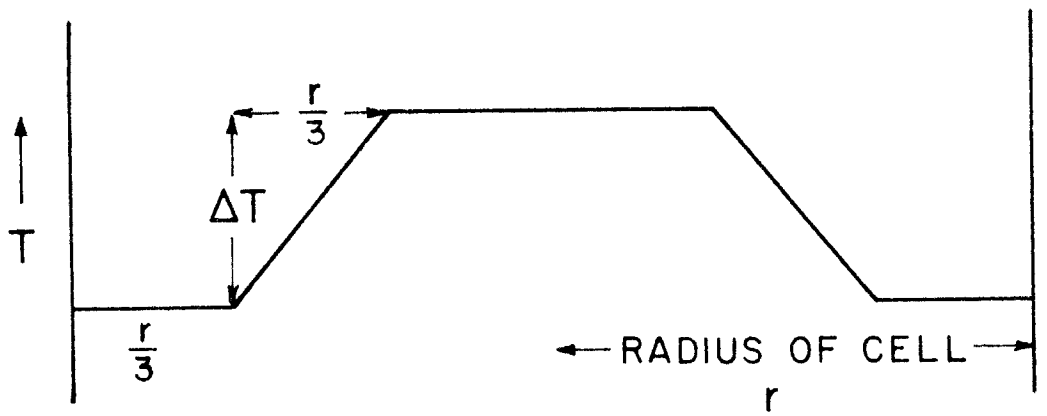

b. Christie, Harrison, Norrish, & Porter

Figure 9. TEMPERATURE PROFILES

(18) $$c_c T_c = c_o T_o = c_c(T+\Delta T) = c_o T$$

with $c_c V_c + c_o V_o$ = n moles of gas;

this follows from the requirement that there be no pressure gradients in the cell.

Elimination of c_o from equations 18 and use of $V = V_o + V_c$ leads to

(19) $$c_c = nT/(VT+V_o\Delta T)$$

so that the fractional change in concentration at the center, $(c_c-c)/c$ where $c = n/V$, is

(20) $$\frac{-V_o\Delta T}{VT+V_o\Delta T} \approx \frac{-V_o\Delta T}{VT} \equiv y.$$

Substitution of (20) in (17) gives

(21) $$y = -2g\,\frac{\sqrt{Dt}}{r}\,\frac{\Delta T}{T} \quad .$$

y is the fractional loss of I_2 from the light path along the axis of the cylinder, and is therefore related to concentrations by

(22) $$y = \frac{[I_2]_{app} - [I_2]}{[I_2]} \quad .$$

This is almost the same as the definition of y in CHNP (p.453). On the concentration brackets in equation 22 and hereafter, "app" means "apparent"; the absence of a subscript implies the concentration that would have prevailed in the absence of heat diffusion effects.

The CHNP model corresponding to the foregoing assumes a temperature profile whose radial part is independent of time. It is illustrated in figure 9b.

Their assumption is evidently equivalent to a stationary step-function similar to that in our calculation, with some $\delta r/r$ in the vicinity of 1/2. Actually CHNP obtain by approximation $y = -0.83\,\Delta T/T$, so that in terms of our model they have chosen $\frac{V_o}{V} \approx \frac{5}{6}$, which is equivalent by geometry to $\frac{\delta r}{r} = 0.592$. According to our treatment this form of correction is applicable only at a time described by

(23) $$g\sqrt{Dt}/r = 0.592;\ t = 0.350\ r^2/g^2D.$$

The consequences of this will be examined in a later paragraph.

The dependence of the apparent rate constant on y must now be computed. From equation 22,

(24) $$[I_2]_{app} = [I_2](1+y);$$
$$[I]_{app} = 2([I_2]_i - [I_2]_{app})$$
$$= 2([I_2]_i - [I_2]\{1+y\})$$

(25) $$= [I] - 2y[I_2].$$

$[I_2]_i$ is the concentration before the flash.

(26) $$[I]_{app}^{-1} = [I]^{-1}\,(1-2y[I_2]/[I])^{-1};$$

which, since $[I] \gg |2y| \cdot [I_2]$, can be written as

(27) $$[I]_{app}^{-1} = [I]^{-1}\,(1+2y[I_2]/[I]).$$

(28) $$\frac{d[I]_{app}^{-1}}{dt} = (1+2y[I_2]/[I])d[I]^{-1}/dt + 2\frac{[I_2]}{[I]^2}\,\frac{dy}{dt} + 2y\,\frac{[I_2]}{[I]}\,\frac{d[I]^{-1}}{dt}\,,\ \text{if } [I_2] \approx \text{constant};$$

with the definitions $S_{app} \equiv d[I]_{app}^{-1}/dt$ and $S \equiv d[I]^{-1}/dt$,

(29) $$S_{app} = (1+4y[I_2]/[I])S + 2([I_2]/[I]^2)dy/dt.$$

The S's are slopes of the kinetic plot; they are proportional to the observed rate constant. The fractional corrections will therefore be the same for both.

Equation 29 can be compared with that appearing on p. 453 of CHNP if the following observations are made. Their expression for $[I]_{app}/[I]$ is inverted, as can be seen by comparing the forms of the top and bottom equations on that page. A factor $1/(1-y)$ has been taken ≈ 1 in deriving their expression for $[I]_{app}/[I]$. If, therefore, y is neglected in comparison to 1 elsewhere in their equation for k_{app}/k, the coefficient of S in equation 29 is obtained. Although CHNP allow y to vary implicitly with time, they do not make the (appreciable) correction represented by the second term of(29).

For convenience in the evaluation of the correction terms equation 29 is rewritten

(30) $S_{app} = S(1+c_1+c_2)$, where

$c_1 = 4y[I_2]/[I]$, the CHNP correction;

$c_2 = (2[I_2]/S[I]^2)dy/dt$, the time variation correction.

To evaluate c_1, the following substitutions with dimensionless variables are made in equation 21 for y;

(31) $C\,\Delta T = \alpha\phi\Delta H$; $\Delta T/T = h\alpha\phi$ with $h \equiv \Delta H/CT$,

where $\phi = [I_2]/[M]$; α= initial degree of dissociation.

ΔH = 60 Kcal/mole as in CHNP; and C = the heat capacity of the third body. The heat capacity used here should be between C_v and C_p; for argon 4 cal/mole is used. Then,

(32) $y = -2gh\alpha\phi\sqrt{Dt}/r$.

The extent of recombination is described by a parameter $\beta = [I]_o/[I]$. $[I]_o$ is I atom concentration just after the flash. Then, $t = (\beta-1)/[I]_oS$. Substitution of this and (32) in equation 30 for c_1 yields

(33) $$c_1 = \frac{8gh\alpha\phi[I_2]}{r[I]}\sqrt{\frac{D_1}{P}\cdot\frac{(\beta-1)}{S[I]_o}},$$

where D has been made pressure-dependent, D_1 being the heat diffusivity at 1 atm pressure. Since $\alpha[I_2] = \frac{1}{2}[I]_o$, (33) can be rearranged to

$$(34) \qquad c_1 = \frac{-4gh\beta\phi}{r}\sqrt{\frac{D_1}{P}\cdot\frac{(\beta-1)}{S[I]_o}} \quad .$$

The estimation of c_2 starts from

$$(35) \qquad dy/dt = -gh\alpha\phi\sqrt{Dt}/rt;$$

substitution of this in (30) gives

$$(36) \qquad c_2 = -2[I_2]\ gh\alpha\phi\sqrt{Dt}/rSt[I]^2 \ .$$

If t in the denominator is written in terms of β , and α is eliminated as before, the result is

$$(37) \qquad c_2 = -\phi gh\sqrt{Dt}\,\beta/r(\beta-1),$$

which is

$$(38) \qquad c_2 = \beta c_1/4(\beta-1).$$

After noting that the total correction c_1+c_2 is always greater than the CHNP correction c_1, we combine the two terms into a single correction C, which, for large β , approaches $5c_1/4$.

(39) $$S_{app}/S = k_{app}/k = 1+C;$$

$$C = c_1(5\beta-4)/(4\beta-4)$$

$$= [\beta(5\beta-4)/4(\beta-1)^{\frac{1}{2}}]x$$

where $$x = (-4gh\phi/r)(2D_1[M]/Pk[I]_o)^{\frac{1}{2}}$$

$$= (-4gh\phi/r)(2D_1/k[I]_oRT)^{\frac{1}{2}};$$ R = gas constant.

x is a function of the experimental conditions only, and the function of β is a universal time factor applicable to all experiments. Some values of the β expression are given in table 1.

Table 1

β	$\beta(5\beta-4)/4(\beta-1)^{\frac{1}{2}}$
1.1	1.30
1.2	1.34
1.3	1.48
1.5	1.86
2.0	3.00
2.5	4.33
3.5	7.47
5.0	13.1
10.0	38.3

The β expression appears to diverge as $\beta \to 1$ ($t \to 0$). This apparition is caused by the initial assumption that the temperature rise occurs instantaneously, and should be disregarded.

x was evaluated for our case and for that of CHNP. For argon the numbers used were $D_1 = 0.33$ $cm^2 sec^{-1}$ at 1 atm pressure, h = 50, g = 2.5; r is 2.5 cm for us and 1.25 cm for CHNP. The results are

(40) $x(\text{Pasadena}) = -0.05 \text{ to } -0.003$

$x(\text{CHNP}) = -.07$ for the plot at the top of p. 448 of the reference.

In our experiments β runs between 1.1 and 3, with the rate constant obtained from the slope of the second-order plot at $\beta = 1.1$, as previously described. Appreciable deviation from linearity is seldom observed in these plots. Evidently these corrections are, as predicted, relatively unimportant for us--especially in view of the approximation that all the heat appears at the beginning. However, they may be significant for CHNP.

In equation 23, the time at which the CHNP correction is approximately applicable was calculated. If expressed in terms of β this condition becomes

(41) $$\beta = 1+0.350\, r^2[I]_o\, S/g^2D$$
$$= 7.6 \text{ (Pasadena)}$$
$$5.9 \text{ (CHNP)},$$

both at a pressure of 100 mm argon. Thus the CHNP model is not applicable to our experiments at all, but is roughly correct for CHNP when their "percent reaction completed" is 83 per cent.

The use of corrections referring to 83 per cent reaction, at earlier stages in the recombination, should lead to overcorrection of the rate constant. It might be anticipated, therefore, that the hypothetical curve in the CHNP plot (Fig. 1, p. 448) should be replaced by one with a less negative slope in the early stages of the reaction but more

nearly vertical when the reaction is nearly complete.

It is difficult to guess, in the absence of specific information about the method of extrapolation used by CHNP, what will be the probable effect of these corrections on the CHNP rate constants. If their rate constants are in error because of faulty thermal correction, the error will be most severe at high values of $[I_2]/[M]$. It will be found useful, in comparing our data with that of CHNP, to examine the possibility that their low pressure rate constants are less reliable than those measured at high pressure.

IV. SPECTROPHOTOMETRY

As stated in the description of the equipment, Corning No. 3486 filters are used between the flash lamp and reaction vessel, and an H-486 interference filter and a Corning No. 3387 filter in the path of the light used to determine I_2 concentration. These sets of filters nominally transmit light in mutually exclusive regions of the spectrum; the purpose of this arrangement is to reduce the influence of flash lamp light on the photomultiplier tube. The filter transmission curves are shown in figure 10a. The crossover wavelength is approximately at the convergence limit at 4995 $\mathring{A}$ in the I_2 spectrum corresponding to dissociation into one normal and one excited iodine atom ($^2P_{3/2}$ and $^2P_{1/2}$). The use of light of longer wave length than this to effect

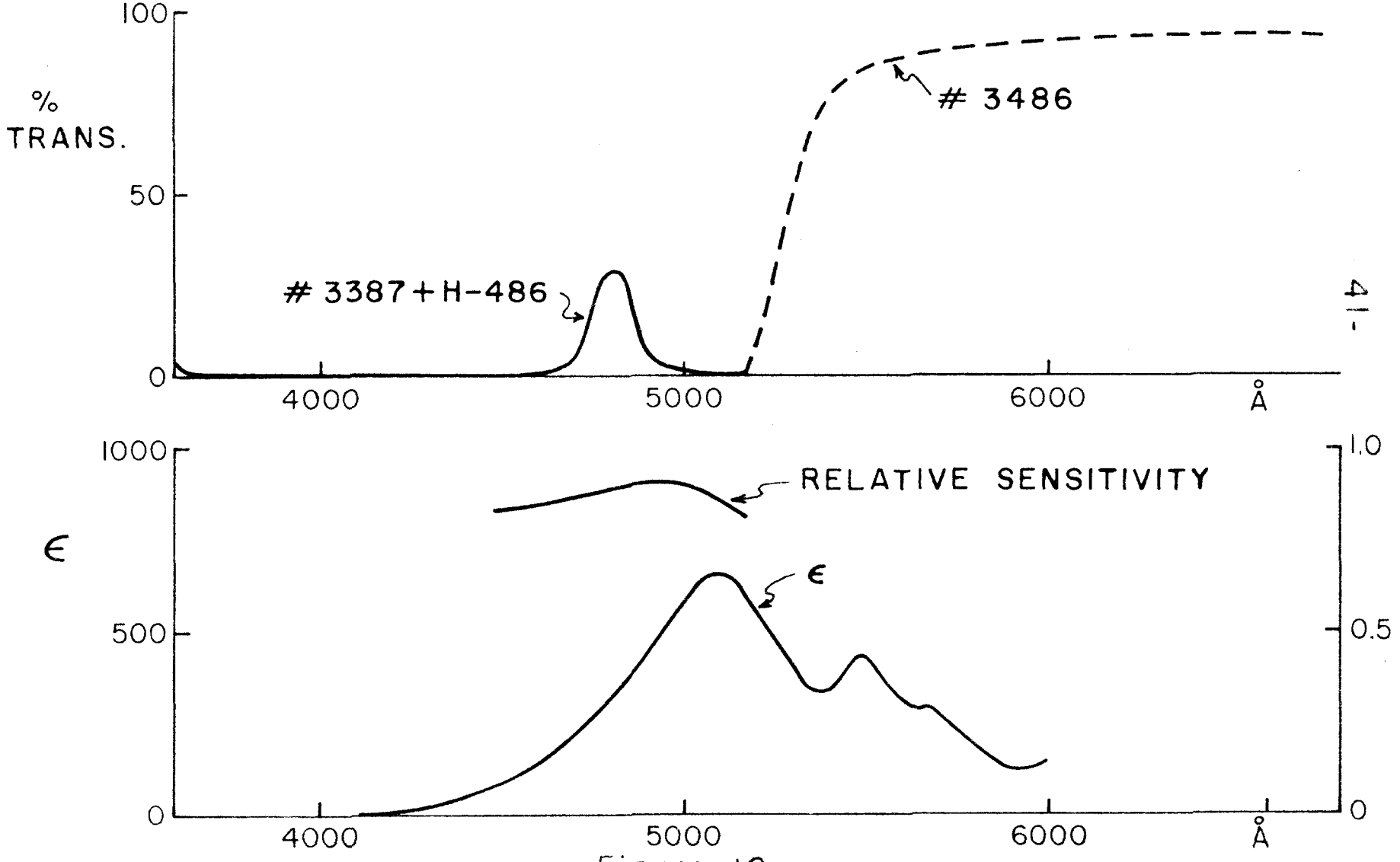

Figure 10.

a. FILTER TRANSMISSION b. EXTINCTION COEFFICIENT OF IODINE

the initial dissociation depends on a pressure-induced predissociation leading to normal atoms. The continuum of the I_2 spectrum, below 4995 Å, is used exclusively for spectrophotometry.

Both the decadic extinction coefficient of I_2 as a function of wavelength at room temperature, and the emission-transmission band of the combination of the photomultiplier, filters and 3200 °K tungsten filament used in these experiments, have been measured in this laboratory (11). These data are shown in figure 10b. A preview of the probable value of ϵ was obtained by graphic methods; the value $\epsilon = 350$ was obtained. The exact extinction coefficients were measured in the apparatus.

Optical density measurements made on I_2 samples vaporized into the cell from the thermostatted U-tube are very reproducible; the difficulty in obtaining reliable extinction coefficients in this way stems from incomplete control of the temperature inside the U-tube and thus of the exact concentration of I_2 in the cell. If there is one atmosphere of argon in the cell and the furnace is appreciably above room temperature, the actual I_2 concentration may be almost twice that expected on the basis of the water bath temperature, even if the thermal siphon is not operated (at high furnace temperatures the hot gases circulate rapidly due to convection). Consequently only "vacuum" extinction coefficient measurements--ones in which only I_2 was present in the cell--were attempted with this method. 20 such

measurements at 50 °C gave an average ϵ of 400. From 12 measurements at 200 °C, obtained with two slightly different configurations of the optical path, ϵ = 390 and ϵ = 381 were determined.

A chemical determination of I_2 concentration was employed in some additional measurements at 50 °C. For these, a temporary double-beam spectrophotometer was constructed, in which one light path was simply the spectrophotometric light path of the apparatus. A second was introduced by placing a half-silvered mirror in front of the converging lens, as in the photomultiplier calibration procedure, except that this time the second light source was another 500 watt tungsten lamp operated from the same bank of storage batteries as the one usually employed. A special cell was constructed, the cylindrical portion of which had the same dimensions as the reaction cell, but which possessed only one small side arm leading to a standard taper joint. A test-tube-like standard taper device was attached thereto, using a bare minimum of silicone stopcock grease in a small ring at the farthest part of the joint from the cell. This apparatus was evacuated, filled with I_2 vapor and sealed off. The intensity of light reaching the photocathode from the two light sources was equalized (this equality being stable for about an hour) and the cell inserted in the furnace. After temperature equilibration the optical density was read and the cell removed. The I_2 was frozen down in the test tube with liquid nitrogen and the cell opened at

the standard taper joint. The I_2 was quantitatively dissolved in KI solution and titrated to a starch end point with standard sodium thiosulfate solution. The solution used was of necessity quite weak (about .002 N) and was restandardized against a carefully prepared (by weighing) I_2-KI solution before and after each titration.

Twelve such measurements, including two with 1 atm argon (which required 12 hours for freezing down of the I_2), yielded the reassuring value $\epsilon = 400$. This established, the extinction coefficient as a function of temperature was determined. For "vacuum" measurements this involved simply heating the furnace from room temperature to 275 °C rapidly enough so that the light beams remained in balance, and recording the optical density and temperature at intervals. Three runs were made in this manner; the result is exhibited in figure 11. The double-beam data fit well with the previous 200 °C measurements, and the whole curve is easily consistent with that reported by Britton (12).

If added gas was present in the cell this procedure could not be used, because at a rate of heating sufficiently slow for continuous temperature equilibrium in the gas, the cell could not be brought to a high enough temperature before the light beam intensities drifted into imbalance. However, the 1 atm extinction coefficient could be determined at a single high temperature by rapidly heating to that temperature and then waiting a short time for equilibrium.

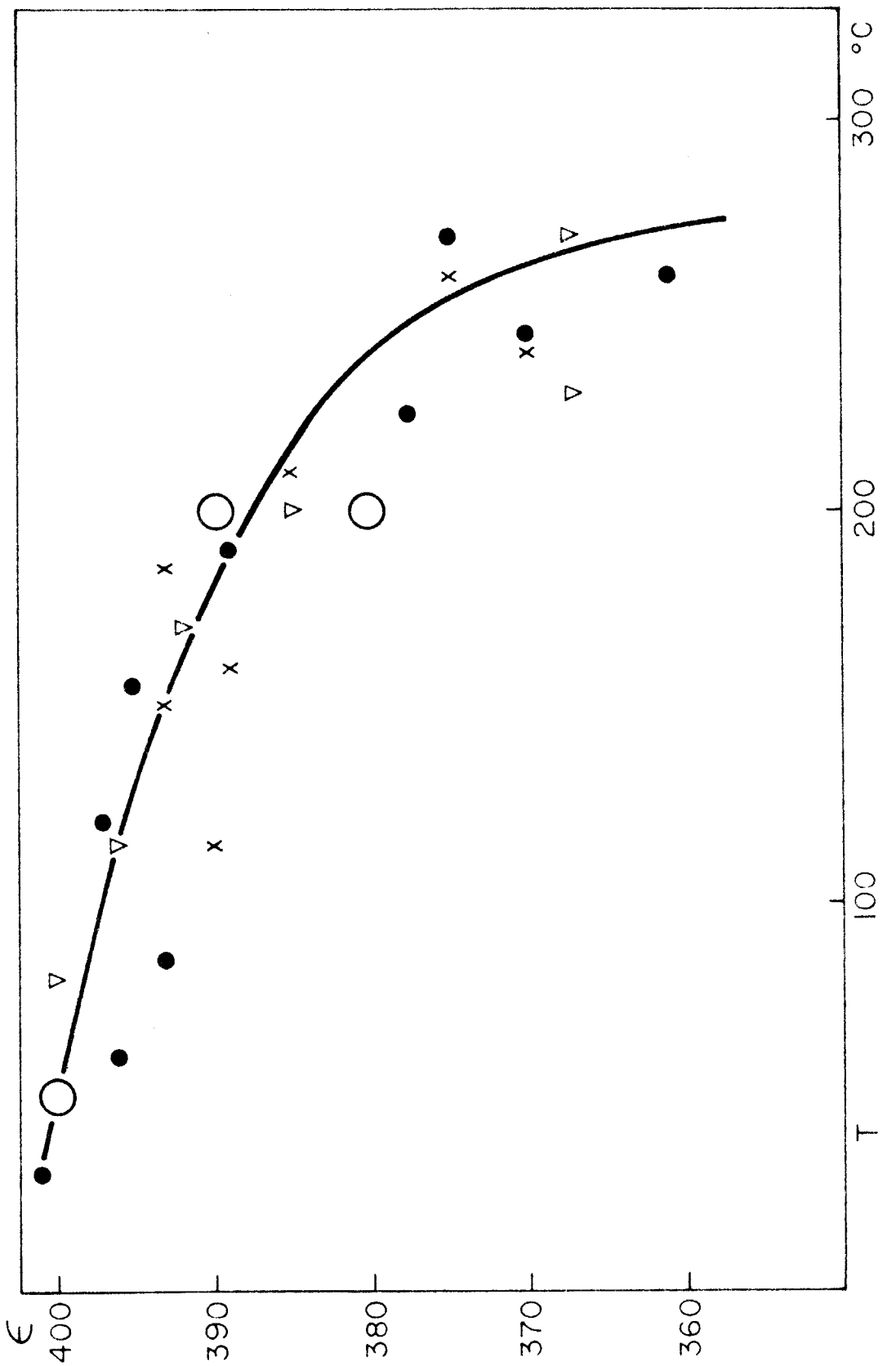

Figure II. EXTINCTION COEFFICIENT OF IODINE

▽ 1st run X 2nd run ● 3rd run ○ Average of isothermal measurements

Invariably the extinction coefficient obtained in this way coincided with that obtainable from figure 11; this test was repeated a number of times for various temperatures. It was concluded that in the range of our experiments the extinction coefficient of I_2 is independent of total pressure, and the data of figure 11 were accepted for use in kinetic calculations.

V. RESULTS

1. Measurements in Argon

All the rate constants determined in this investigation are displayed in table 2.

In the major phase of the research, the added gas was Linde argon, supplied 99.99 per cent pure and passed over Drierite before use. The measurements described in section III-1 were performed at temperatures of 29, 50, 100, 150, 200, and 275 ^{o}C.

The plots of the observed rate constants vs $[I_2]/[A]$ at these temperatures are shown in figure 12. The observation that k(A,50) is greater than k(A,29), as given by the intercepts, is not serious in view of the experimental uncertainty. The 29 ^{o}C points at high $[I_2]/[A]$ are beginning to show the calculated deviation due to the thermal effect.

In order to obtain a set of 25 ^{o}C rate constants for comparison with the current results of Christie, Harrison, Norrish and Porter (6) and Strong, Chien, Graf and Willard (7), it is next necessary to obtain a functional relation

TABLE 2

RATE CONSTANTS FOR I+I+M

	T °C	k(M,T)	$k(I_2,T)$
M = Argon			
	29	$(2.72\pm.13)\times10^{9}$	$(2.11\pm.18)\times10^{12}$
	50	$(2.99\pm.13)\times10^{9}$	$(1.07\pm.18)\times10^{12}$
	100	$(2.01\pm.08)\times10^{9}$	$(4.42\pm.42)\times10^{11}$
	150	$(1.66\pm.05)\times10^{9}$	$(1.43\pm.38)\times10^{11}$
	200	$(1.50\pm.06)\times10^{9}$	$(9.6\pm3.0)\times10^{10}$
	275	$(1.13\pm.11)\times10^{9}$	$(12.3\pm8.2)\times10^{10}$
M = n-Butane			
	32	$(3.36\pm.16)\times10^{10}$	$(1.73\pm.22)\times10^{12}$
	100	$(2.17\pm.2)\times10^{10}$	$(2.5\pm1)\times10^{11}$
	220	$(1.20\pm.10)\times10^{10}$	$(1.79\pm.22)\times10^{11}$
M = Hydrogen			
	53	$(4.43\pm.08)\times10^{9}$	$(1.20\pm.05)\times10^{12}$
M = Deuterium			
	52	$(3.97\pm.04)\times10^{9}$	$(7.54\pm.22)\times10^{12}$

Units are liters^{2}mole^{-2}sec^{-1}. Limits shown are approximately the probable error of the least squares fit to $k(M,T) = k(M,T \text{ observed}) + k(I_2,T)[I_2]/[M]$.

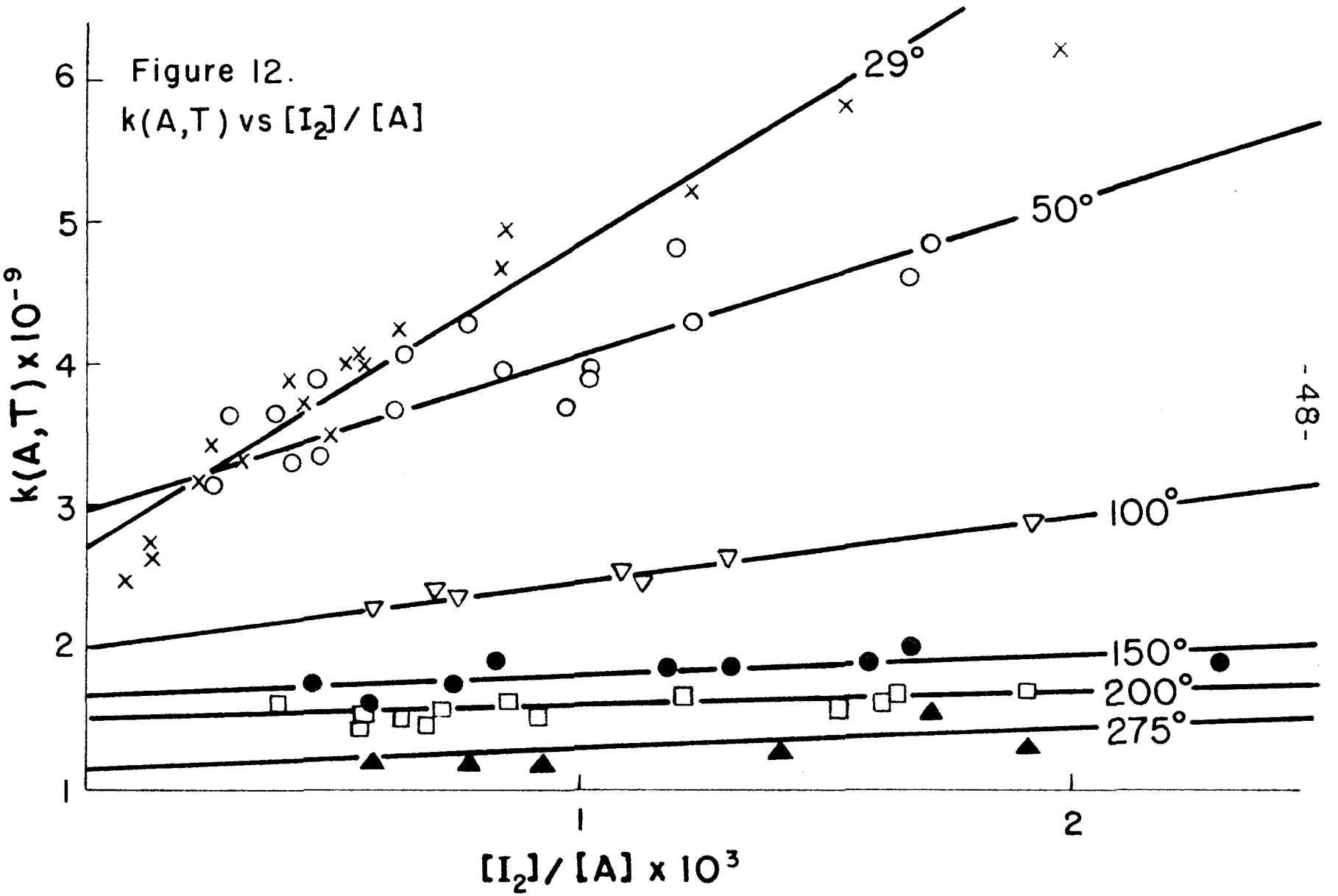
Figure 12.
k(A,T) vs [I2] / [A]
29°
50°
100°
150°
200°
275°
k(A,T) x 10-9
[I2] / [A] x 10³
1
2
3
4
5
6
1
2

between $k(A,T)$ and T, and also $k(I_2,T)$ and T.

In anticipation of the functional form required for interpretation, $\ln[k(I_2,T)/T^{3/2}]$ is plotted against $1/T$ in figure 13. This representation is selected so that the rate constant may be resolved into the product of a collision number and an equilibrium constant. It will be convenient later if the equilibrium constant in pressure units is of the form $Ae^{E/RT}$ where A and E are more or less constant. This requires that the concentration equilibrium constant have the temperature dependence $Te^{E/RT}$ and that the rate constant in concentration units vary with temperature as $T^{3/2}e^{E/RT}$.

In this plot the values of the rate constant measured with 3 other gases besides argon, are included. As predicted, the $k(I_2,T)$ seem to fit the same relationship regardless of what the added gas was. A weighted least squares fit gives

$$(42) \qquad k(I_2,T^{\circ}K) = 10^{4.65}T^{3/2} \exp(5.32 \text{ Kcal}/RT).$$

In the discussion of $k(A,T)$ accompanying the shock tube investigation, two methods of presenting temperature dependence data were employed (13). Similar ones are also used here. In figures 14 and 15 $\ln[k(A,T)/T^{3/2}]$ and $\log_{10}[k(A,T)]$ are correlated with $1/T$ and $\log_{10} T$ respectively. The recent findings of Willard et al. (7) are also displayed but are not included in the least squares fit, which uses $k(A,T)$ from table 2 and, in the case of log k vs log T, from the

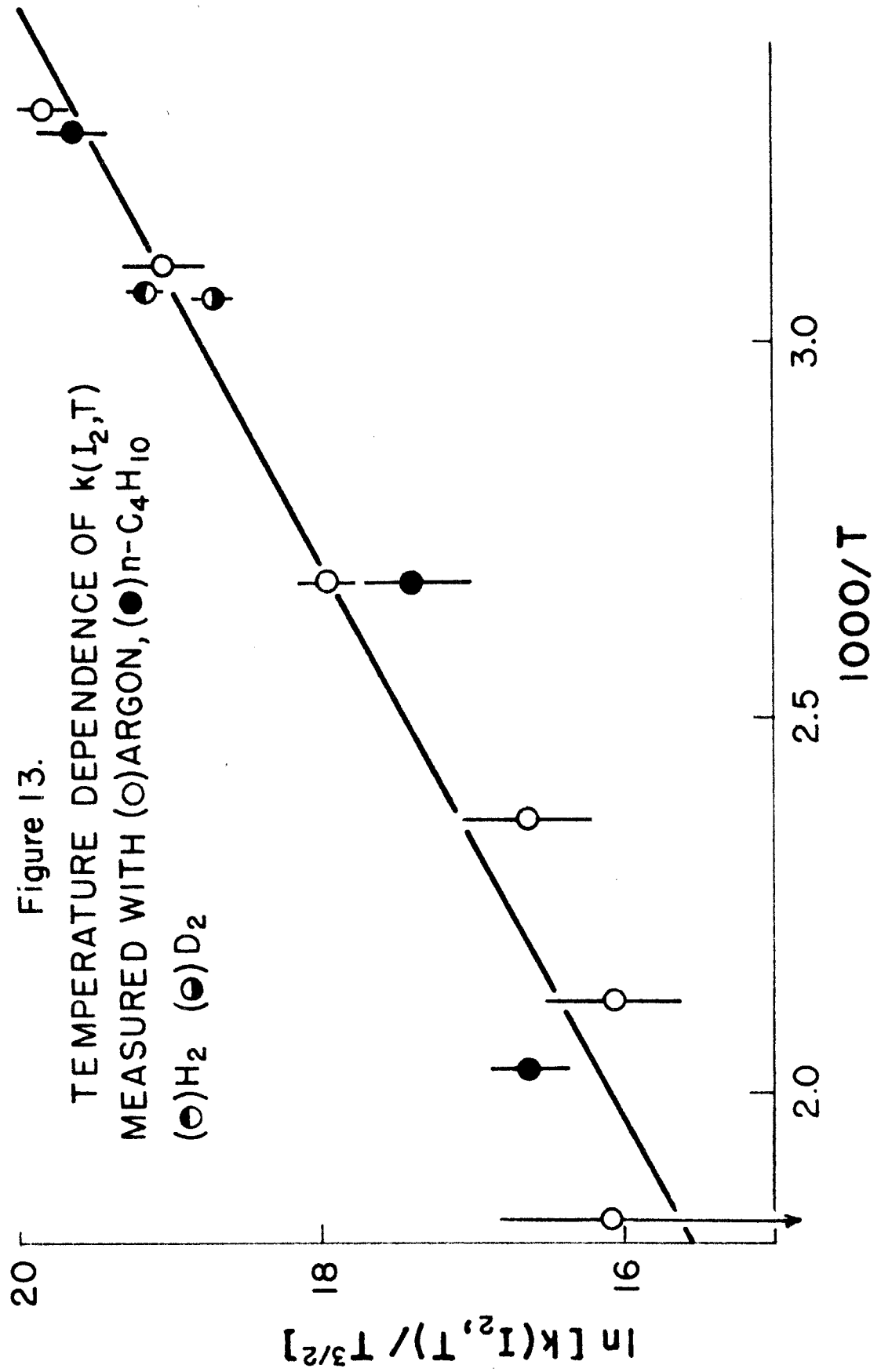

Figure 13.
TEMPERATURE DEPENDENCE OF $k(I_2,T)$
MEASURED WITH (○)ARGON, (●)n-C_4H_{10}
(◐)H_2 (◑)D_2

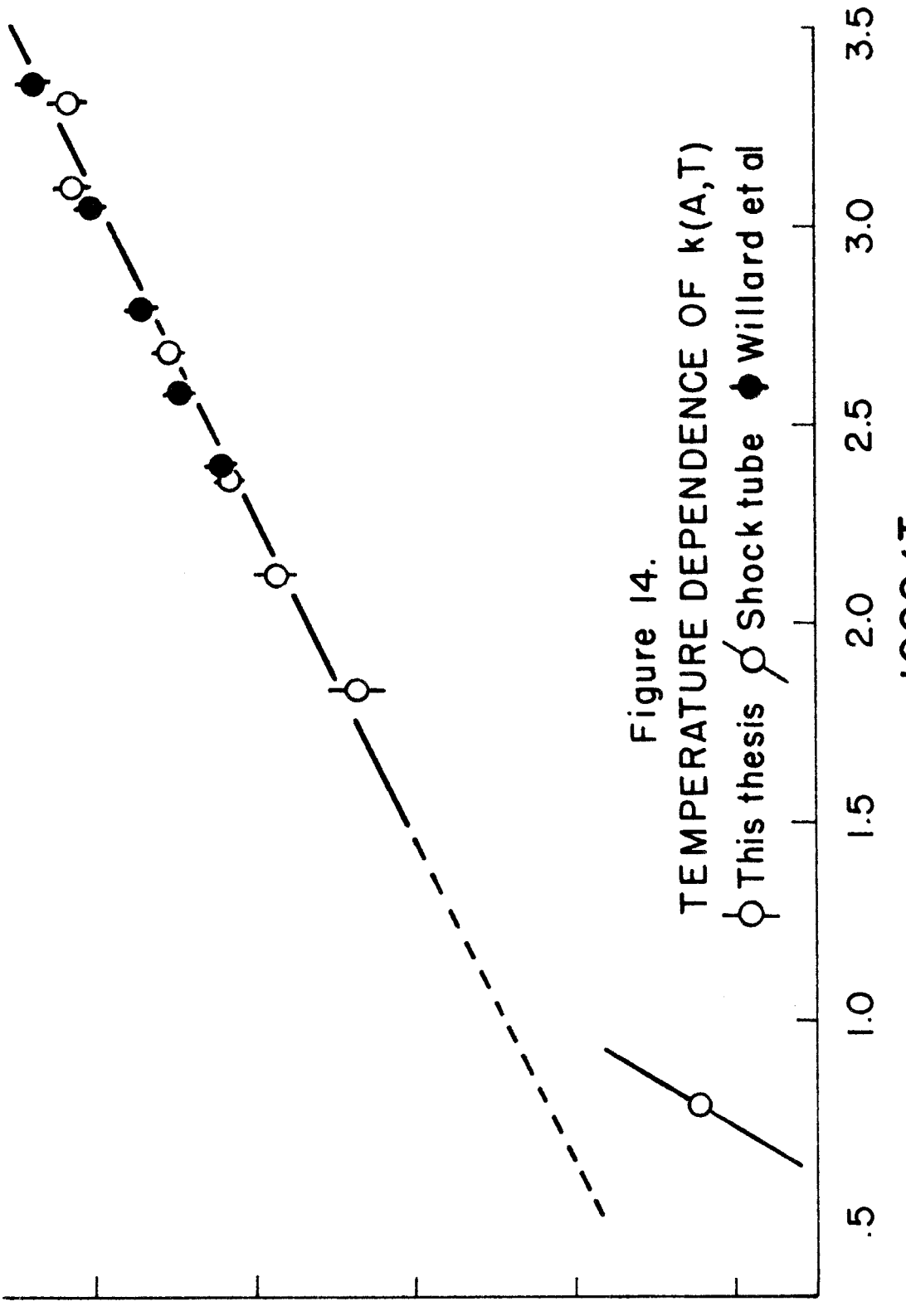
ln [k(A,T) / T^3/2]
13
12
11
10
9
.5
1.0
1.5
2.0
2.5
3.0
3.5
1000/T
TEMPERATURE DEPENDENCE OF k(A,T)
This thesis
Shock tube
Willard et al

Figure 14.

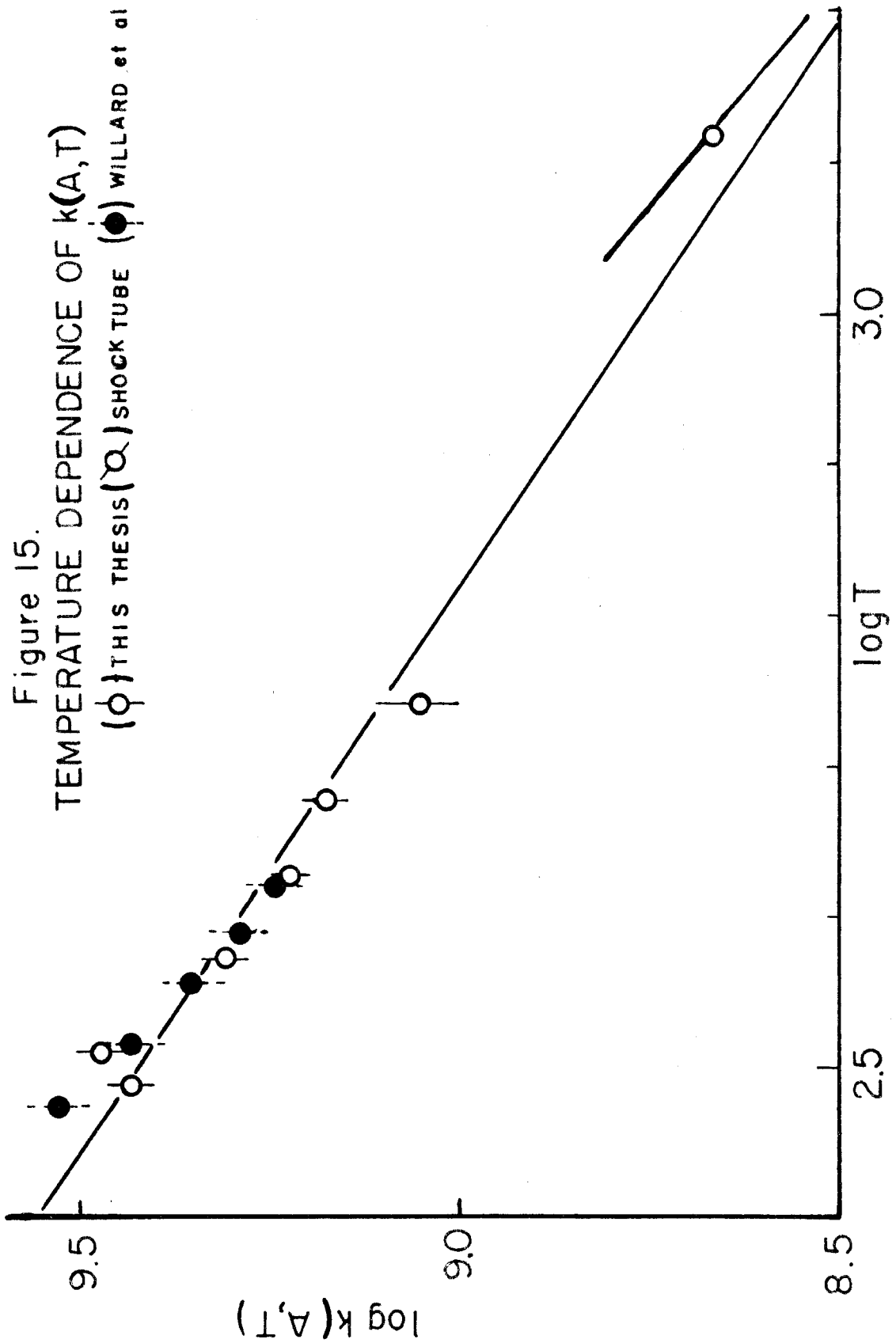

Figure 15.
TEMPERATURE DEPENDENCE OF k(A,T)
(○) THIS THESIS (○) SHOCK TUBE (●) WILLARD et al

shock tube results (14). The shock tube data are treated in the log-log calculation as a single point at 1285 ^{o}K, where $k(A, 1285\ ^{o}K) = 10^{8.665}$. Willard's points are slightly uncertain because his apparatus seems to have yielded, in alternate years, two distinct sets of data for the same experimental conditions. The "high" and "low" values thus obtained differ by about 20 per cent. This discrepancy is neither very large nor very serious for the purposes of the present comparison. In figures 14 and 15, the range shown for the Willard rate constants has as its extremes the equivalent "high" and "low" values. The agreement between the data reported here and Willard's rate constants is remarkably good.

The functional relations so obtained are

(43) $k(A,T^{o}K) = 10^{4.00}T^{3/2}\exp(2.45\ \text{Kcal}/RT)$ from fig.14;

(44) $k(A,T^{o}K) = 10^{12.75}T^{-1.33}$ from fig. 15.

From equations 42-44 the rate constants $k(A,25)$ and $k(I_2,25)$ pertaining to this investigation may be computed. The results are

(45) $k(I_2,25) = 1.88 \times 10^{12}$

$k(A,25) = 3.26 \times 10^{9}$ from equation 43;

2.85×10^{9} from equation 44.

In figure 16 these numbers are compared with the Christie, Harrison, Norrish and Porter (6) and Strong, Chien, Graf and

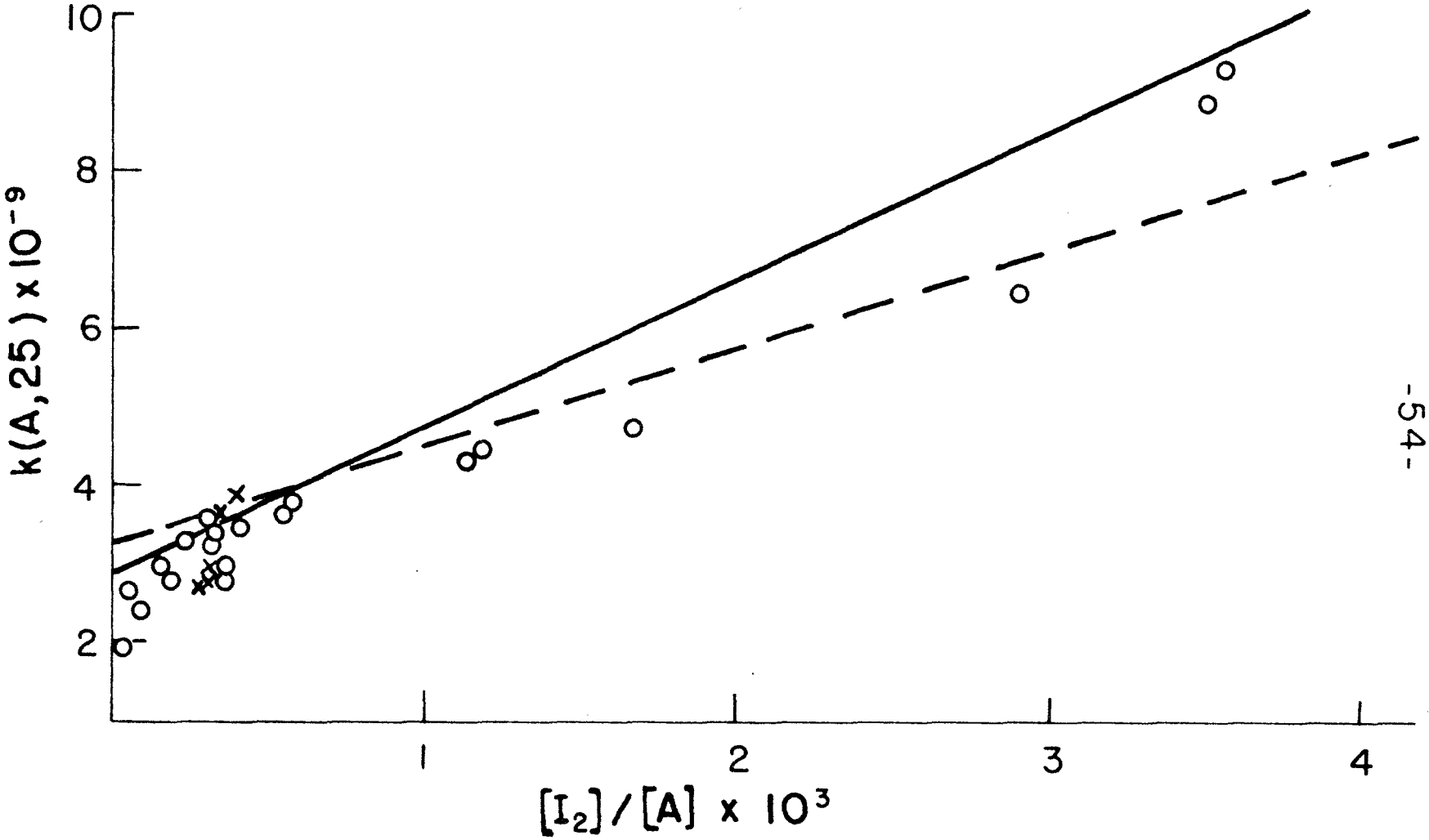

Figure 16. k(A,25°C) vs $[I_2]/[A]$

(o---o) Porter et al, (x) Willard et al, (——) This thesis

Willard (7) data. The points shown correspond to those of figures 7 and 3 of the references, respectively. The lower value of k(A,25) in equation 45 is used in this plot. The "tail" portion of the straight line of Porter et al. is omitted.

The three investigations seem to be in agreement that the "best value" of the room temperature rate constant is close to 3.0×10^9. This agreement is approximately within the predicted errors of the three investigations, so that the discrepancy which led to this investigation can probably be regarded as removed.

The agreement between the slopes of the Porter line and the data reported here is fair. If the Porter slope is entered as a point on figure 13, it is noticeably but not calamitously low. Abandonment of the Porter procedure of neglecting the points in the "tail" (in figure 16, all those circles below $[I_2]/[A]$ approximately 0.35×10^{-3}) would result in quite good agreement; the argument developed in section III-3, that Porter's most reliable points may be those in the "tail," could be used to support this. Because of the much greater volume of data, figure 13 and equation 42 should probably be regarded as giving the "best" value of $k(I_2,25)$.

2. Measurements in n-Butane

The studies in n-butane were initiated chiefly in order to provide a check on the $k(I_2,T)$ determined in argon.

The n-butane was obtained in pure form through the courtesy of the Chemical Engineering Department of the California Institute, and was redistilled once in the course of transfer to the apparatus. It was stored as a liquid in glass at -78 °C, or for longer periods at room temperature under its vapor pressure of about 3 atm. Measurements were made at three temperatures: 32, 100 and 220 °C. The results are included in table 2.

Figure 17 shows the $k(n\text{-}C_4H_{10},T)$ vs $[I_2]/[n\text{-}C_4H_{10}]$ plots obtained at these temperatures; the temperature dependence of the intercepts is examined in figure 18. The dependence of the rate constant on temperature is expressed in the same way as for argon. The straight lines, established by eye, correspond to

$$(46) \qquad k(n\text{-}C_4H_{10},\ T^\circ K) = 10^{4.80} T^{3/2} \exp(2.80\ \text{Kcal}/RT)$$
$$\text{or } k(n\text{-}C_4H_{10},\ T^\circ K) = 10^{15.90}\ T^{-2.16} \quad .$$

A comparison exists between these data and that of Russell and Simons (2). They employed, among other things, propane and n-pentane as third bodies; while the rate constants they measured may be inaccurate due to neglect of $I+I+I_2$, the ratios between them should be reliable. They observed

$$(47) \qquad k(C_3H_8,\ 20^\circ C)/k(A,\ 20^\circ C) = 8.4;$$
$$k(n\text{-}C_5H_{12},\ 20^\circ C)/k(A,\ 20^\circ C) = 13\ ,$$

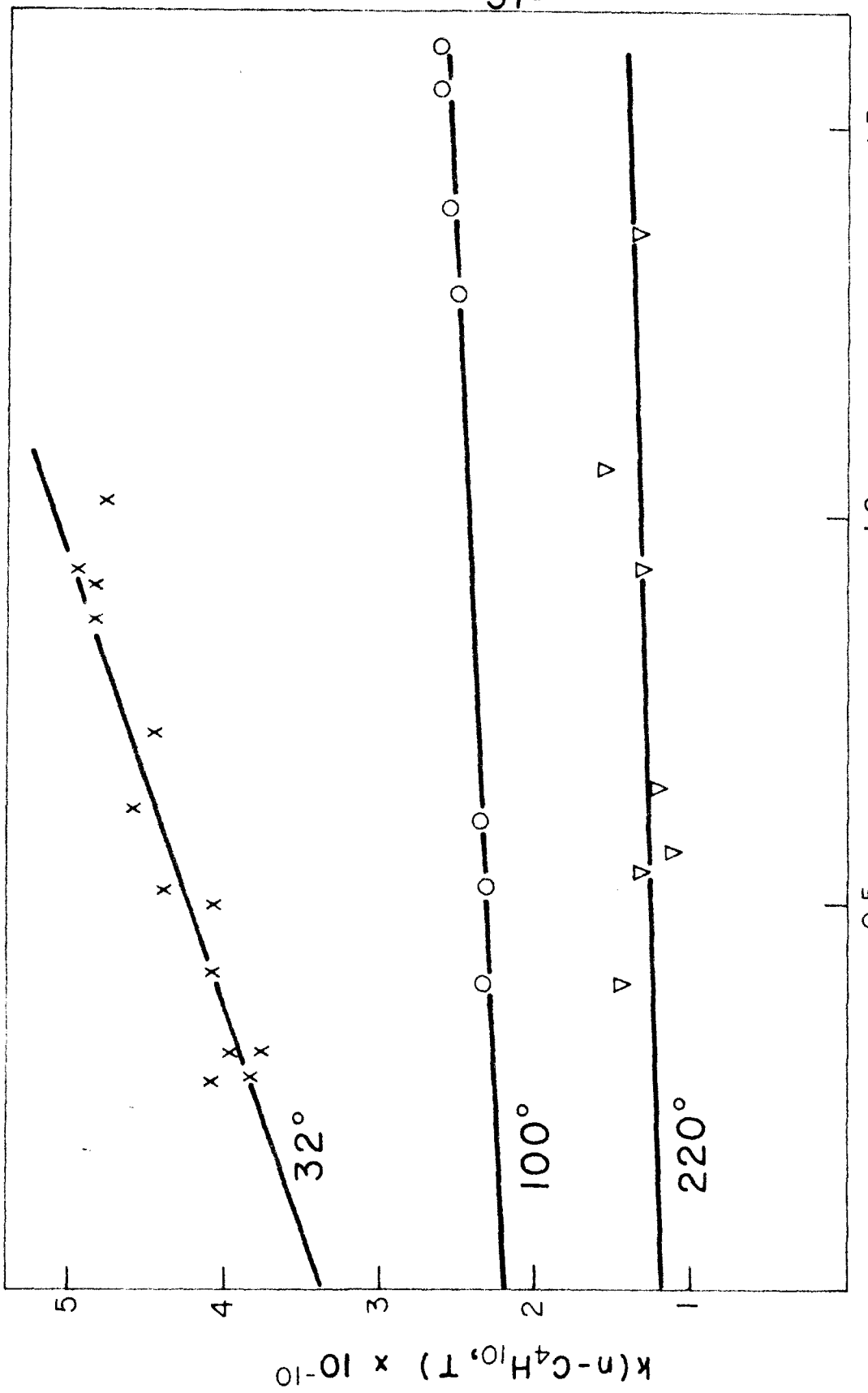

Figure 17. $k(n\text{-}C_4H_{10}, T)$ vs. $[I_2]/[n\text{-}C_4H_{10}]$

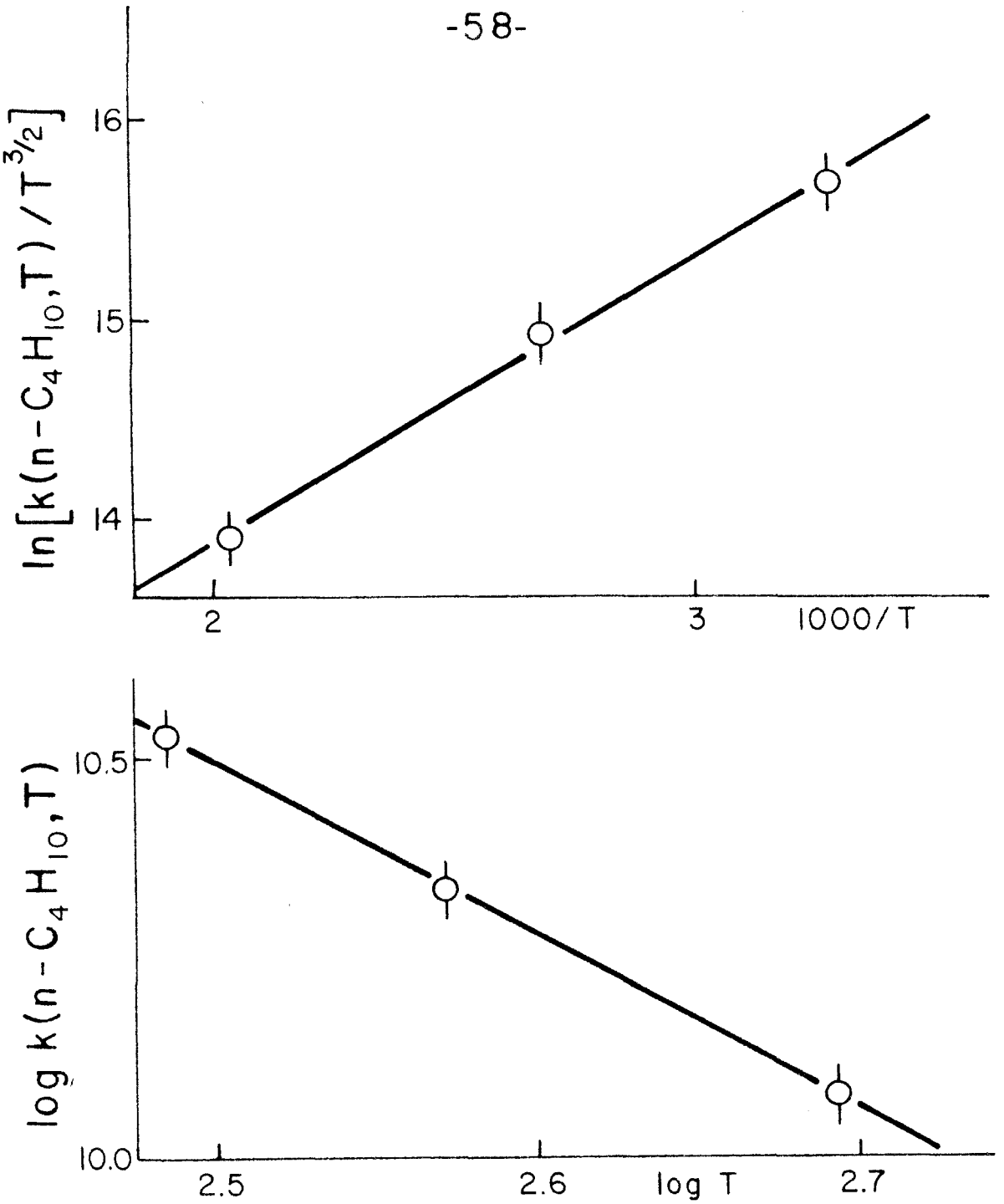

Figure 18.

TEMPERATURE DEPENDENCE OF $k(n\text{-}C_4H_{10}, T)$

whereas the measurements reported here lead to approximately

(48) $k(n\text{-}C_4H_{10}, 20^{\circ}C)/k(A, 20^{\circ}C) = 13$,

in reasonably good agreement.

3. Measurements in Hydrogen and Deuterium

The third-body efficiencies of hydrogen and deuterium were compared at a single temperature, 53 °C. The materials used were 99.9 per cent pure Linde hydrogen, and deuterium supplied by the Stuart Oxygen Company and stated to be of >99.5 per cent purity.

The results are exhibited in the usual way in table 2 and figure 19. The ratio $k(H_2,53)/k(D_2,53)$ is 1.11. Some difficulty was experienced in these measurements with misbehavior of the furnace temperature controlling system, and it is likely that the divergence of slopes in figure 19 reflects a difference in furnace temperature of approximately 5°. If the temperature dependences of $k(H_2,T)$ and $k(D_2,T)$ are roughly similar to the others measured in this investigation, a correction for this 5° error may be calculated. The use of this correction reduces the above ratio of rate constants to about 1.04.

The rate constant for hydrogen may also be compared with data of Russell and Simons. The work reported here leads to a $k(H_2,53^{\circ}C)/k(A,53^{\circ}C)$ of about 1.5; Russell and Simons reported 1.3 for the same ratio at $20^{\circ}C$.

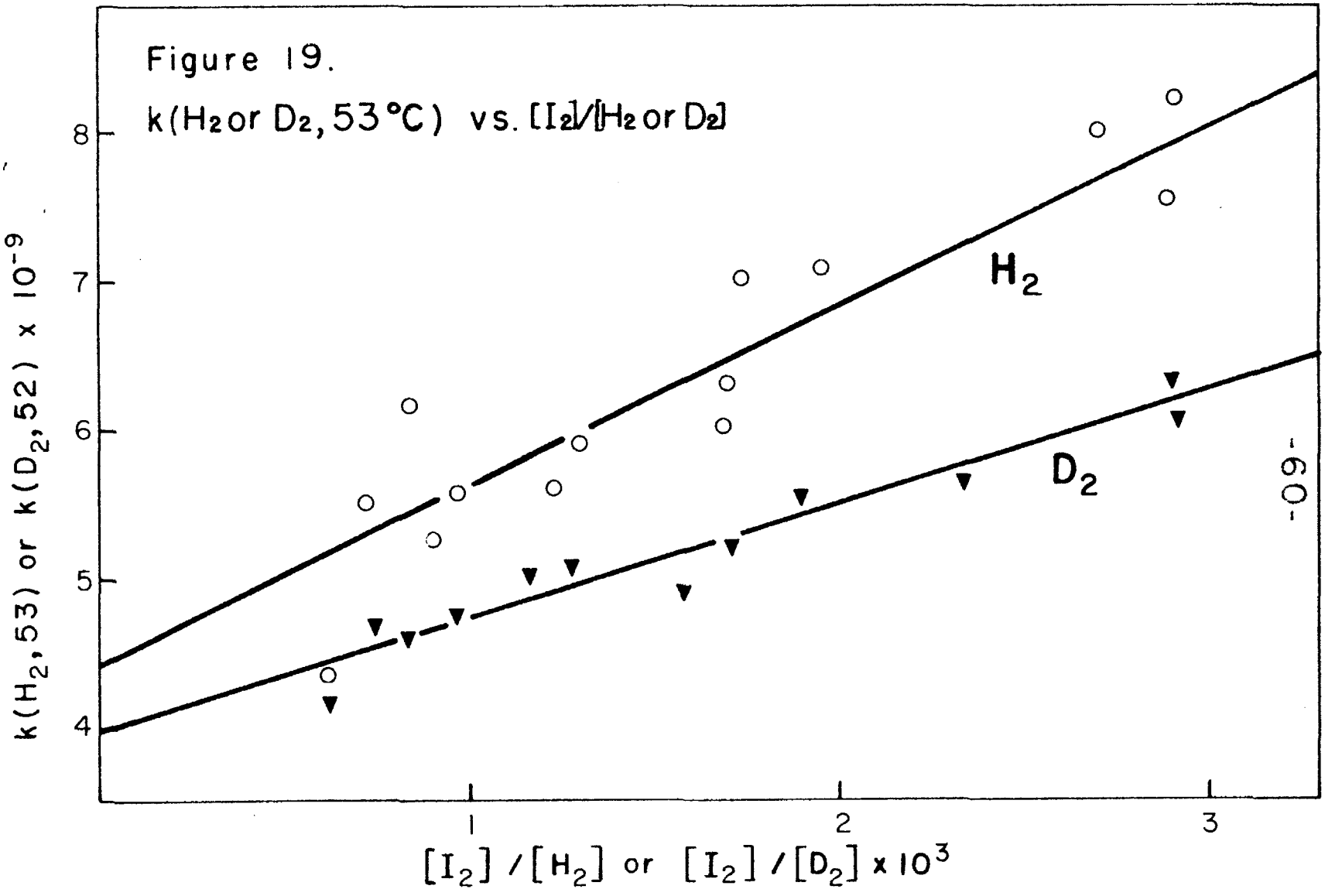
Figure 19.
k(H2 or D2, 53°C) vs. [I2]/[H2 or D2]
H2
D2
-09-
k(H2, 53) or k(D2, 52) x 10-9
[I2] / [H2] or [I2] / [D2] x 10^3
4
5
6
7
8
1
2
3

VI. DISCUSSION

1. Introduction

Interpretation of the data is facilitated if the overall reaction

(49) $$I+I+M \longrightarrow I_2+M$$

can be subdivided into two bimolecular processes. Although the proper method of doing this is not at first apparent, two limiting cases may be discussed.

If the added gas if perfect, or if the object M is idealized as a hard sphere, the only possible mechanism of recombination is

(50) $$I+I \rightleftharpoons I_2^*$$

$$I_2^*+M \longrightarrow I_2+M$$

and the rate of recombination should be a function only of the temperature and the mass and radius of M. At the other extreme, if M interacts strongly enough with I atoms to form an intermediate species eligible for designation as a chemical compound, the mechanism would be expected to be

(51) $$I+M \rightleftharpoons IM$$

$$IM+I \longrightarrow I_2+M \ .$$

In the second case the relative efficiency of M is largely regulated by the detailed nature of the interaction potential between I and M. These two limiting mechanisms do not constitute an "either-or" choice for the recombination of I atoms in, say, argon; initially, one must entertain the

prospect that the true course of events may be intermediate between the above two alternatives.

The observed rate constant for either mechanism is given by

(52) $$k = PZK \quad ,$$

where K is the equilibrium constant for the first step, and Z and P are a collision number and steric factor referring to the second step if its activation energy is zero.

2. Evidence for IM: $k(I_2)$, $k(H_2)$ and $k(D_2)$

A prime example of the circumstances which lead to the second type of mechanism is the reaction

(53) $$I+I+I_2 \longrightarrow 2I_2 \quad ,$$

for which the rate constants $k(I_2,T)$ are reported here. That this reaction realizes the conditions for the IM mechanism is demonstrated by the extreme efficiency of I_2 as a third body, and by the existence of precedent for the postulation of trihalogen compounds (IM = I_3).

By semiempirical methods Rollefson and Eyring (15) estimated the stability of the trihalogen molecules. For the reaction

(54) $$I+I_2 \rightleftharpoons I_3$$

they calculated an equilibrium constant

(55) $$K(I_3) = 0.003 \exp(2.4 \text{ Kcal}/RT)$$

in pressure units. The assumptions which led to this preferred result were (a) that the bond energies are 10 per cent coulombic, in analogy with theoretical results for

the hydrogen molecule, and (b) that since the entropy change involved in the halogen association reactions ($2X \rightleftharpoons X_2$) is about 20 entropy units, ΔS° for halogen reactions of the form (54) is between 0 and -20 e.u. and is probably about -12 e.u. They also observed, from a qualitative inspection of the potential surfaces involved, that trihalogen molecules would be expected to have lifetimes equal to many times their periods of vibration.

Trihalogen molecules have been postulated in a number of reaction mechanisms, both before and after the appearance of the Rollefson and Eyring analysis. Many of these are listed by Steacie (16). Unfortunately, it is difficult to distinguish, in an ordinary photochemical investigation, between halogenation reactions initiated by atoms and by trihalogen radicals. Steacie concludes only that (for construction of halogenation mechanisms) trihalogen is "unnecessary."

The equilibrium constant $K(I_3)$, as estimated in this investigation, may be used to evaluate the possible contribution of I_3 in iodination reactions.

This equilibrium constant is obtained from equations 42 and 52, with the assumption that P = 1. In the calculation of the collision number, the value $\sigma_{I_3\text{-}I} = \sigma_{I_2\text{-}I_2} = 5$ Å was used. The result is

(56) $$K(I_3) = k(I_2,T)/Z$$
$$= 6.33\times10^{-6}\ T \exp(5.32\ \text{Kcal/RT})\ \text{liter mole}^{-1}$$
$$= 7.7\times10^{-5} \exp(5.32\ \text{Kcal/RT})\ \text{atm}^{-1}\ .$$

Calculation of the ratio $[I_3]/[I]$ in saturated I_2 vapor at room temperature yields the value 3×10^{-4}; this decreases as the temperature is raised. Evidently I_3 is not an important intermediate except when (as in this investigation) an abnormally high concentration of atoms is present.

For the reaction $I+I_2 \rightleftharpoons I_3$, the form of (56) in pressure units is equivalent to the thermodynamic statements

(57) $\Delta H^\circ = -5.32$ Kcal

$\Delta S^\circ = -20.2$ e.u. ;

if the steric factor P is not 1, then ΔS° is to be corrected by addition of the positive number $(-R \ln P)$. This correction is rather small.

For the reaction

(58) $I+I \rightleftharpoons I_2$

one calculates from the N. B. S. tables (17) $\Delta S^\circ = -24$ e.u. The result (57) thus conforms to the spirit of the assumption (b) of Rollefson and Eyring.

A somewhat more specialized estimate of ΔS° may be obtained by regarding I_3 as a linear half-bonded molecule and making an approximate statistical calculation of its entropy at 298°K. The bond length may be taken as 2.75 Å by Pauling's rule (18). Standard methods lead to the results

(59) $S_{trans} = 43.7$ e.u.

$S_{rot} = 20.6$ e.u.

$S_{elect} = 2.7$ e.u. ,

the latter if the electronic degeneracy of I_3 resembles that

of I. The vibrational calculation, however, leads to considerable uncertainty.

The stretching force constants may be approximated by use of the equation of Gordy (19), which allows the nominal bond order to be included in the calculation. There is no Gordy or Badger type of rule which applies to bending modes. Inspection of data given in Herzberg's text (20) reveals that for triatomic molecules the bending frequencies tend to be about half the symmetric stretching frequencies, corresponding in various cases to bending force constants about an order of magnitude smaller than stretching force constants. In the absence of other criteria, this observation was used to complete the set of frequency guesses

(60)
$$\nu_1 \cong 120 \text{ cm}^{-1}$$
$$\nu_2 \cong 80 \text{ cm}^{-1} \text{ (doubly degenerate)}$$
$$\nu_3 \cong 210 \text{ cm}^{-1} ,$$

from whence

(61)
$$S_{vib} = 13.1 \text{ e.u.}$$
$$S = 80.1 \text{ e.u.}$$

From this estimate, one obtains for the reaction under discussion (equation 54), $\Delta S^\circ = -25$ e.u., in reasonable agreement with the observations. The analogous formation of ozone from O_2 and O has $\Delta S^\circ = -30$ e.u. (17). Thus both the interpretation of $k(I_2,T)$ and the measured energetics of formation of I_3 appear to be relatively plausible.

The results of the measurements in hydrogen and deuterium are consistent with the IM mechanism. The equili-

brium constant for the formation of the intermediate IM should not depend on whether M is H_2 or D_2. The collision number Z for IM+I is also practically independent of M in this case. However, if the I+I mechanism of equation 50 applies, the collision number between I_2^* and M differs by a factor of $2^{1/2}$ according to whether M = H_2 or M = D_2. It is necessary to make the rather arbitrary suggestion that the slower moving D_2 is more effective than H_2 in deactivating I_2^* by a factor of $2^{\frac{1}{2}}$ per collision, in order to explain the results on the latter basis. Thus the comparison of H_2 and D_2 tends to favor the IM mechanism.

3. The Measurements in Argon and Butane

The results of the measurements in which the rate of recombination was determined over a large range of temperature do not lend themselves to easy interpretation. In the first place, the exact form of the observed temperature dependence law is quite uncertain; since the rate of recombination in the presence of argon shows only a sixfold decrease when the temperature is raised by 1000°, it is not surprising that a fairly wide variety of k = f(T) expressions are compatible with the data. Furthermore, even with this latitude in the choice of an observed temperature dependence, it is not possible to reconcile the observations with the behavior predicted by simple calculations based on the possible mechanisms given above. For each type of calculation, one or more purely speculative assumptions are

required in order to obtain agreement with the data. In this section, some of these calculations and their modes of failure are examined.

In the hard sphere treatment, the equilibrium constant K for $I+I \rightleftharpoons I_2^*$ is taken as proportional to the lifetime of I_2^* and the rate of its formation (a collision number). The lifetime τ is approximated as the vibration period of I_2 in the lowest vibrational level of its ground electronic state; thus $\tau \cong 1/(c \cdot 216\ cm^{-1})$. The calculated rate constants are

$$k = Z_{I-I}\,\tau\,P Z_{I_2-M} \tag{62}$$

$$= 1.6 \times 10^9 (T/298) P \text{ for M = argon;}$$

$$= 2.7 \times 10^9 (T/298) P \text{ for M = butane.}$$

Collision diameters were taken or estimated from Hirschfelder (21). The observed rate constant for butane is 13 times that for argon, whereas the calculation gives only a factor of 1.7. Making τ larger by increasing the lifetime of I_2^* over that given by the vibration period would improve the magnitude of the rate constants but not their ratio.

The above treatment suggests that the rate of recombination should increase with temperature, in contradiction to equations 44 and 46. The steric factor P, in order to remove this contradiction, must vary as about $T^{-5/2}$ for argon and T^{-3} for butane.

Construction of a rate constant from the IM mechanism

requires equilibrium constants for the formation of the quasi-molecules I·A and $I \cdot C_4H_{10}$. These can be obtained by adapting the procedure used for estimating the second virial coefficient of a mixture of imperfect gases.

Following Pitzer (22), the concentration equilibrium constant for formation of IM is written in terms of classical partition functions;

$$(63) \qquad K = VQ_{IM}/Q_I Q_M$$

$$= Q_{int}(m_{IM}/m_I m_M)^{3/2}(h^2/2\pi kT)^{3/2}$$

if the usual translational partition functions are inserted.

$$(64) \quad Q_{int} = \frac{h^{-3}}{\sigma}\int\cdots\int \exp\left[-\left(\frac{p_x^2}{2\mu} + \frac{p_y^2}{2\mu} + \frac{p_z^2}{2\mu} + \epsilon[r]\right)/kT\right] dp..dq..$$

σ, the symmetry number, is <u>one</u>. Each of the momentum integrals is $(2\pi\mu kT)^{1/2}$. If the configurational part of the integral is shifted to polar coordinates and the angles integrated, the result is

$$(65) \quad Q_{int} = 4\pi(2\pi\mu kT/h^2)^{3/2} \int_0^{r_1} \exp(-\epsilon[r]/kT)r^2dr \ .$$

r_1 is the internuclear distance at which a "molecule" is said to have been formed. Substitution of (65) in (63) cancels the mass expressions and leaves

$$(66) \quad K = \frac{4\pi N}{1000}\int_0^{r_1} \exp(-\epsilon[r]/kT)r^2dr \qquad \text{liter mole}^{-1} \ .$$

The factor N/1000 (N = Avogadro's number) has been introduced in order to change the units from cc atom^{-1} to liter mole^{-1}.

The Lennard-Jones potential function is used:

$$(67) \qquad \epsilon[r] = \epsilon_o[(r_o/r)^{12} - 2(r_o/r)^6] \quad .$$

The integral in equation 66 need not be evaluated, as it has in effect already been computed in the construction of tables of second virial coefficients. The expression for the second virial coefficient is

$$(68) \quad B = \frac{2\pi N}{1000} \int_o^\infty [1 - \exp(-\epsilon[r]/kT)]r^2 dr \qquad \text{liter mole}^{-1}.$$

From (68) and (66),

$$(68a) \quad B = 2\pi(N/1000)r_1^3/3 - K/2 + 2\pi(N/1000) \int_{r_1}^\infty [1 - \exp(-\epsilon[r]/kT)]r^2 dr \quad ,$$

so that

$$(68b) \quad K = -2B + 4\pi(N/1000)r_1^3/3 - 4\pi(N/1000) \int_{r_1}^\infty [1-\exp(-\epsilon[r]/kT)]r^2 dr \quad .$$

B, the second virial coefficient, is itself negative when the attractive forces between molecules are important.

The distance r_1 at which a molecule IM is said to be

formed is not well defined. Presumably r_1 is slightly greater than r_o. The last integral in equation 68b is negative, and is customarily neglected in the calculation of virial coefficients. We make the approximation that

(69) $K = -2B + 4\pi(N/1000)r_o^3/3$,

that is, that the sum of the terms $4\pi(r_1^3 - r_o^3)/3$ and

$4\pi\int_{r_1}^{\infty}[1-\exp(-\epsilon[r]/kT)]r^2dr$ may be neglected.

The place where the Lennard-Jones potential is zero is called σ, and is given by $r_o = 2^{1/6}\sigma$. The usual tabulations give B/β, where $\beta = 2\pi(N/1000)r_o^3/3$ liters mole^{-1}. Equation 69 may be rewritten in its final form,

(70) $K = \frac{4}{3}\pi\sigma^3(N/1000)\ (\sqrt{2} - B/\beta)$ liter mole^{-1} ,

where B/β is to be looked up in tables (23).

For the purpose of interacting with argon, iodine atoms are regarded for the present as similar to xenon. The required Lennard-Jones parameters are estimated (21,24) with the aid of the rules

(71) $$\epsilon_o^{IM} = (\epsilon_o^{XeXe}\epsilon_o^{MM})^{1/2}$$

$$\sigma_{IM} = (\sigma_{XeXe} + \sigma_{MM})/2.$$

The numbers so obtained are

(72) $(\epsilon_o^{IA}/k) = 164$ $(\epsilon_o^{IC_4H_{10}}/k) = 259$

$\sigma_{IA} = 3.73$ Å $\sigma_{IC_4H_{10}} = 4.97$ Å ;

these values can be used with equation 70 to obtain a graphic relation between K and T, and thus between $k = PZ_{I-IM}K$ and T. The collision numbers used are

(73) $$Z_{I-IA} = 10.4 \times 10^{10} (T/298)^{1/2}$$

$$Z_{I-IC_4H_{10}} = 16.6 \times 10^{10} (T/298)^{1/2} \quad .$$

The result of all these calculations is displayed in figure 20, along with the observed results (taken from figure 15) for comparison. On this kind of plot, a parallel displacement of the calculated curve from the observed would indicate error in a constant, such as σ or the steric factor P. P is taken as 1 in the figure. An angular discrepancy between the curves indicates that the steric factor, in order to take up the difference, must again vary according to some power of T. This variation, measured from the figure, amounts to close to $T^{-3/2}$ for both argon and butane. The extreme values of P are about 1/5 and 1/80.

Various refinements can be made to this calculation, such as using other criteria to estimate σ, or allowing it to be regulated by the position of the rotation barrier in the I-I(A) collision; these effect moderately large changes in the magnitude or temperature dependence of the

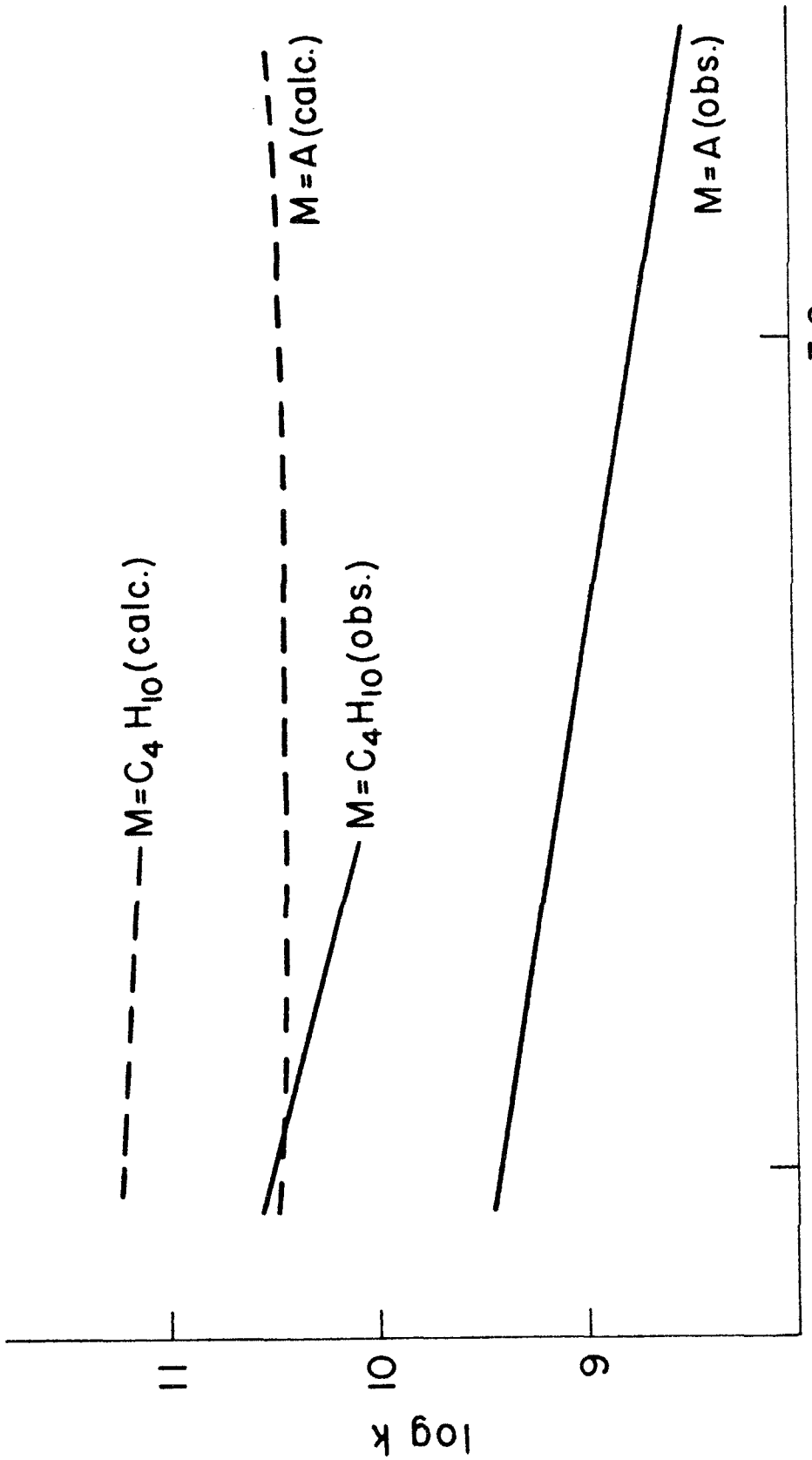

Figure 20. OBSERVED vs. CALCULATED RATE CONSTANTS

number which must be assigned to P in order to superimpose the calculated results on the observed. However, the lack of concrete knowledge of what behavior should be expected of P reduces the usefulness of these modifications.

An alternate interpretation of the results may be obtained by scrapping the procedure used in equations 71-72 for estimating the magnitude of the interaction between I and M, and assuming instead that the actual interaction is described by the energies

(74) $$\epsilon_o^{IA} = 2.45 \text{ Kcal}$$

$$\epsilon_o^{IC_4H_{10}} = 2.80 \text{ Kcal}$$

derived in equations 43 and 46 from the experimental data. These values are outside the range of the Lennard-Jones treatment, so an argument similar to that used for $M = I_2$ must be employed. If equations 43 and 46 are divided by the collision numbers of equation 73 and the steric factor P, and the resulting equilibrium constants shifted to pressure units, the result is

(75) $$K(IA) = (2 \times 10^{-5}/P)\exp(2.45/RT)$$

$$K(IC_4H_{10}) = (8 \times 10^{-5}/P)\exp(2.80/RT).$$

A very rough calculation of the entropy of IA, following the procedure used for I_3, gives $\Delta S = 0$ to -10 e.u., which would indicate that P is in the range of about $10^{-3\pm1}$. This

smaller P is to be expected if the stronger interaction is assumed. The method of presenting the data used here (i.e. $\ln kT^{-3/2}$ vs T^{-1}) carries the implicit assumption that P does not vary appreciably with temperature.

Validation of this interpretation depends on breaking down the assumption that the iodine atom, with its odd electron, is no more attractive to argon than is xenon. The attractive part of the Lennard-Jones potential varies approximately as the square of the polarizability of the molecule. If for the mixed case the energy is assumed to vary as

$$E \sim \left[(\alpha_I + \alpha_A)/2\right]^2 \tag{76}$$

then the relation between the actual polarizability of xenon, and that which apparently should be assigned to iodine atoms, is

$$\alpha_{I,obs}/\alpha_{Xe} \cong 3 \quad . \tag{77}$$

There is a method for calculation of approximate polarizabilities by summing contributions from electrons in the various shells of atoms (26), with an "effective nuclear charge" assigned to each shell from screening constants. Calculation of the polarizability of xenon by this method gives $\alpha_{Xe} = 2.0 \times 10^{-24}$ cm^3; the observed value is 4.0×10^{-24} cm^3. The same type of calculation yields

(78) $$\alpha_{I,calc} / \alpha_{Xe,calc} = 1.5 \quad .$$

This leaves only a factor of 2 unaccounted for.

To summarize these calculations: Each method of prediction of rate constants requires that specific restrictions be imposed on the steric factor P. If the mechanism involving I_2^* prevails, P is between 1 and 0.1 at room temperature and decreases very rapidly (as $T^{>2}$) as the temperature is raised; and the unexpected requirement that $P(A) \gg P(C_4H_{10})$ is encountered. If the reaction is considered to proceed via the intermediate IM, then to the extent that IM resembles a Van der Waals complex P is in the range 0.1-0.01 and decreases as $T^{-3/2}$. If the interaction between I and M is for some reason stronger than anticipated, then the temperature dependence requirement on P is eased and its value may be as low as 0.001.

A somewhat different approach to the problem of calculating the rate constant for the reaction $I+I+A \rightarrow I_2+A$ is being made elsewhere (25). It is modeled after the compound nucleus theory of nuclear reactions. The calculation proceeds generally by assuming that the phase space available to the system I, I, A has uniform probability after their collision and calculating the fractional volume thereof which is accessible to I_2+A. The preliminary results are that the rate constant increases as $T^{1/2}$ at low temperature, then levels off and eventually falls as

$T^{-3/2}$. The scale of temperatures, however, has not been determined.

4. Iodine Recombination and Energy Transfer

Russell and Simons (2) plotted their 31 rate constants for different added gases against the boiling point of the added gas. They found a smooth increase in rate constant with boiling temperature, with certain (high rate constant) exceptions: aromatic hydrocarbons, ethyl iodide, and, to a lesser extent, ethyl bromide.

This investigation lends some support to their view, in making this plot, that the degree of interaction of M with I (rather than, for example, the number of oscillators in M) should largely determine the third body efficiency of M. The exceptions listed above are apparently those species capable of forming, with I atoms, a complex more stable than the usual Van der Waals association. Ethyl iodide is a particularly striking example of this; it is at least 4 times as effective as would be expected.

The considerations which lead to the formulation of the equilibrium constant for IM (equation 70) would suggest that a good correlation should exist between $k(M)\mu_{IM-I}^{\frac{1}{2}}/\sigma^3$ and B/β as obtained from the Lennard-Jones parameters for M. The factor σ^{-3} removes the σ dependence of the equilibrium constant in the IM mechanism, allowing B/β alone to be compared with k. The factor $\mu_{IM-I}^{\frac{1}{2}}$ removes the mass dependence of the collision number, so that rates may be compared on

a collision-per-collision basis. The cross section terms of the collision numbers are assumed to vary slowly with M. The correlation is shown in figure 21, with Russell and Simons rate constants, for the gases for which data (21) are available. Hydrogen and benzene would not be expected to fit this plot, and are omitted.

Before an attempt is made to compare iodine recombination data with the results of other energy transfer investigations, a careful specification of the reverse process is in order. The symbol I_2^* has been used here to represent a molecule excited above its level of dissociation, i.e. one which will inevitably come apart if no stabilizing collision occurs. The product of the reaction $I+IM \rightarrow I_2+M$ is almost certainly vibrationally activated, perhaps to within a few kT of dissociation. This molecule will be denoted by I_2^{act}. In a gas mixture at equilibrium in which I_2 is being thermally dissociated, the possible processes according to this system are

(79)

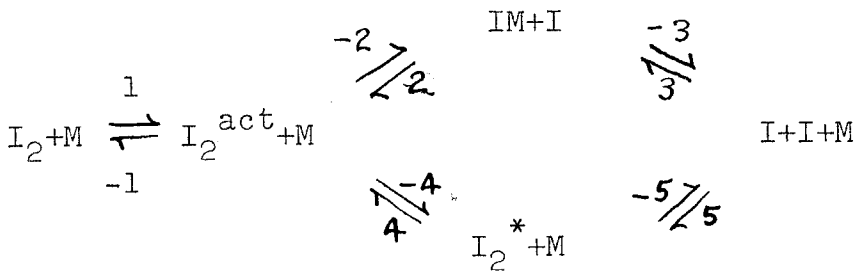

There are, of course, a whole series of states I_2^{act}. If it is assumed, for the sake of argument, that the recombi-

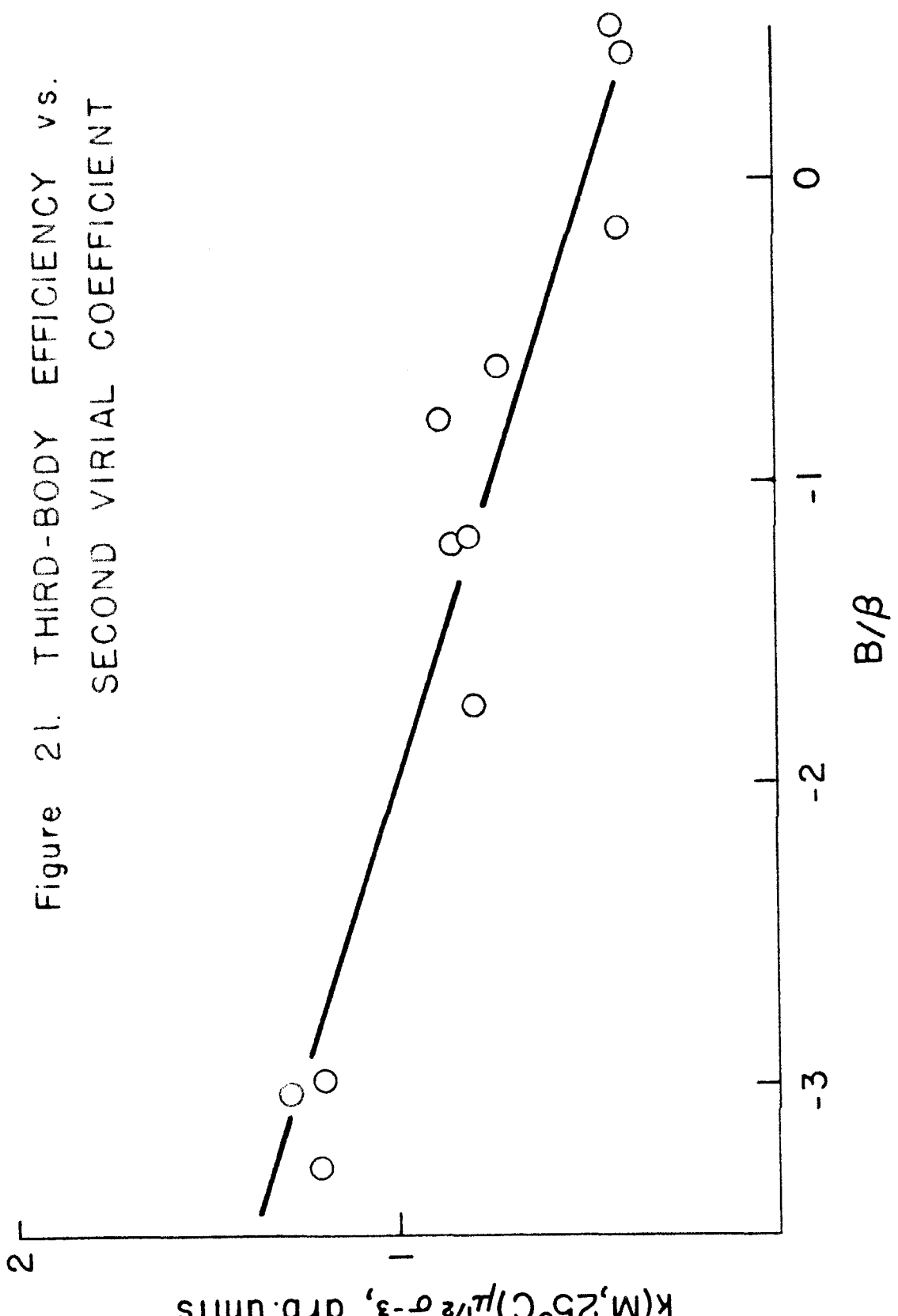

Figure 21. THIRD-BODY EFFICIENCY vs. SECOND VIRIAL COEFFICIENT

nation proceeds mostly by steps (3) and (2), then microscopic reversability requires that the dissociation take place via (-2) and (-3) rather than (-4) and (-5).

While not necessarily taking place at every collision, step (-1) is probably efficient enough that I_2^{act}, once formed, does not again dissociate. Therefore steps (-2) and (-3), whose rates depend on the nature of M, are rate determining for the dissociation process. On the other hand, the rate of step (1) is the quantity of interest in the typical investigation of energy transfer in which unimolecular reactions are studied at low pressures.

In the event M is an "ordinary" gas--free of special interactions with I atoms--it should have almost the same ability to activate I_2^{act} to a higher vibrational state as to form IM+I. For these cases the computed reverse reaction rate for I_2+M should approximately index the efficiency of M in step (1). The above limitations suggest that M should not be allowed to be an iodine-containing substance or an aromatic compound in the comparison to follow.

Volpe and Johnston (27) measured the relative collision-per-collision efficiencies of various gases in the activation of nitryl chloride. The comparison between their results and the Russell and Simons set of rate constants should be of interest; a number of gases were common to both investigations. A relative collision per collision rate constant for I_2+M may be obtained from

$$(80) \qquad k(\text{Dissocn., rel.}) = k(\text{Recomb.})\mu_{I_2\text{-}M}^{\frac{1}{2}} \quad ,$$

since the equilibrium constant involved is the same for all M. Figure 22 shows the comparison. The gases are arranged in the order of their boiling points. Solid circles are the rate constants given by equation 80, in arbitrary units; open circles, data of Volpe and Johnson based on unit efficiency for nitryl chloride; the other points display a second specimen of comparison data, that of Pritchard, Sowden and Trotman-Dickinson (28), obtained by studying the activation of cyclopropane towards isomerization.

The agreement of the iodine data with the conclusions of Volpe and Johnson is satisfactory; agreement with the cyclopropane results is not as good. The cyclopropane data are of a lower order of precision that the other results shown in figure 22. Also, as Volpe and Johnston point out, the cyclopropane data were obtained in the "fall-off" region (the pressure regime where the behavior of a unimolecular reaction is intermediate between first and second order), and may not be strictly comparable with results obtained under actual second-order conditions.

5. Conclusions

In attempting to discover the factors regulating the rate of combination of atoms, the investigator has at his disposal two principal variables: the nature of the third

Figure 22.

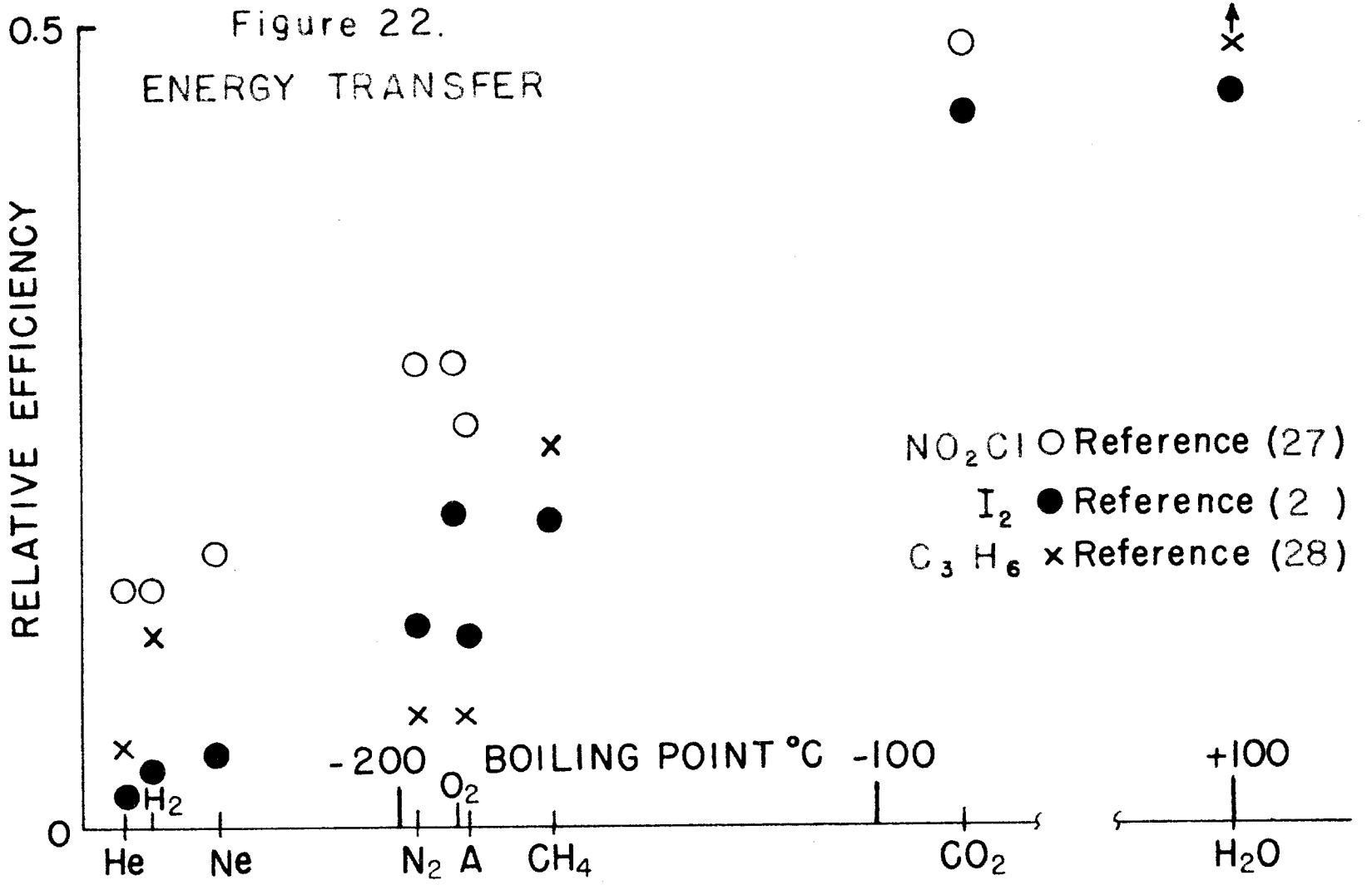
ENERGY TRANSFER
0.5
0
RELATIVE EFFICIENCY
NO_2Cl ○ Reference (27)
I_2 ● Reference (2)
C_3H_6 × Reference (28)
-200
BOILING POINT °C
-100
+100
H_2
O_2
He
Ne
N_2
A
CH_4
CO_2
H_2O

body M, and the temperature. It would appear, from the preceding section, that the problem of understanding the effect of varying M in a recombination process is parallel to that of forecasting the energy transfer properties of M in any other reaction. Thus the interpretation of the effect of the nature of M on the recombination rate is on as firm a basis as can be expected at the present time.

Beyond possible contributions to the state of the art of flash photolysis, this investigation addresses itself to the more difficult problem of elucidating the temperature dependence of atom combination reactions. The measurements in argon, over the large temperature range afforded by combining this work with the shock tube results, comprise the first set of data sufficiently extensive to be useful as a basis for speculation about the dynamics of the process. The main obstacle to interpretation of this data is the lack of a method of estimating the efficiency of the bimolecular process (whatever it is) which yields the final products. Without such an estimate, one cannot even establish that the rate of recombination reactions should decrease with increasing temperature.

Neither can it be said that this investigation determines the sequence in which simpler events combine to produce an apparently termolecular process. It has certainly been shown that if M has a chemical interaction with I atoms, the recombination is most likely to proceed via the intermediate IM; our measurements of $k(I_2,T)$ and certain

of the results of Russell and Simons lend support to this contention. The evidence given here that the reaction always proceeds in this way (regardless of the identity of M) is indicative but not conclusive. The comparison of the effectiveness of H_2 and D_2 as third bodies, while attractive, possesses a loophole through which its usefulness as a test of mechanism could be attacked. If such an attack is to be successful, it requires a particular assumption about the effect of the mass of M on its effectiveness in deactivating I_2^*; this assumption, at present, would be no more nor less speculative than those employed in attempting to establish the IM mechanism. Minor points in favor of the IM system are its greater success in accounting for ratios of rate constants for different M, and the fact that it affords a slightly more satisfying comparison with the observed temperature dependence data.

Although temperature dependence data for the rate of recombination of iodine atoms in the presence of hydrogen, deuterium, ethyl iodide and hydrogen iodide would be of considerable interest, the observations in argon are probably both adequate and most convenient for testing of theoretical treatments of the recombination process. Most of the questions raised in the discussion of the argon results cannot be resolved by further experiments with present fast reaction techniques. Thus it seems that the major features of the behavior of argon as a third body must remain in the

category of unexplained observations, to await the availability of an adequate method of calculating the mechanics of the collision processes involved.

REFERENCES

1. R. Marshall and N. Davidson, J. Chem. Phys. 21, 659 (1953).

2. K. E. Russell and J. Simons, Proc. Roy. Soc. A 217, 271 (1953).

3. M. I. Christie, R. G. W. Norrish and G. Porter, Proc. Roy. Soc. A 216, 152 (1953).

4. M. I. Christie, R. G. W. Norrish and G. Porter, Disc. Faraday Soc. No. 17, 1954, p. 107.

5. D. Britton, Thesis, California Institute, 1955.

6. M. I. Christie, R. G. W. Norrish and G. Porter, Proc. Roy. Soc. A 231, 446 (1955).

7. R. L. Strong, J. C. W. Chien, P. E. Graf and J. E. Willard, in press.

8. R. Marshall, Thesis, California Institute, 1954, p. 26.

9. Ibid., p. 23.

10. Cf. for example RCA 1P22 data sheet and references therein. Radio Corporation of America, Harrison, N. J., 1945.

11. D. Britton and W. DeMore, private communication.

12. D. Britton, Thesis, p. 24.

13. Ibid., pp. 39-40.

14. Ibid., p. 48; D. Britton, N. Davidson, W. Gehman and G. Schott, J. Chem. Phys. 25, 804 (1956).

15. G. K. Rollefson and H. Eyring, J. Am. Chem. Soc. 54, 170 (1932).

16. E. W. R. Steacie, "Atomic and Free Radical Reactions," 2nd. Ed., Reinhold Publishing Company, New York, 1954, Vol. 1 p. 408 ff., and Vol. 2 p. 657.

17. "Selected Values of Chemical Thermodynamic Properties," National Bureau of Standards, Washington, D.C., Series III, 1954.

18. L. Pauling, J. Am. Chem. Soc. 69, 542 (1947).

19. W. Gordy, J. Chem. Phys. 14, 305 (1946).

20. G. Herzberg, "Infrared and Raman Spectra of Polyatomic Molecules," D. Van Nostrand Company, Inc., New York, 1945, p. 160 ff., 172 ff.

21. J. O. Hirschfelder, C. F. Curtiss, and R. Byron Bird, "Molecular Theory of Gases and Liquids," John Wiley and Sons, Inc., New York, 1954, pp. 1110-1112.

22. K. S. Pitzer, "Quantum Chemistry," Prentice-Hall, Inc., New York, 1953, Chap. 11.

23. J. O. Hirschfelder, C. F. Curtiss, and R. B. Bird, op. cit., pp. 1114-1115.

24. E. Whalley and W. G. Schneider, J. Chem. Phys. 23, 1644 (1955).

25. J. Keck, private communication.

26. J. O. Hirschfelder, C. F. Curtiss, and R. B. Bird, op. cit., pp. 951-955.

27. M. Volpe and H. S. Johnston, J. Am. Chem. Soc. 78, 3903 (1956).

28. H. O. Pritchard, R. G. Sowden, and A. F. Trotman-Dickenson, Proc. Roy. Soc. 217 A, 563 (1953); cf. also A. F. Trotman-Dickenson, "Gas Kinetics," Academic Press, Inc., New York, 1955, p. 84.

PROPOSITIONS

1. In connection with the peculiar results obtained by Burwasser and Taylor (1) in their investigation of the photolysis of acetic anhydride, it is suggested that:

(a) Their quantum yield measurement may be in error;

(b) A further attempt should be made to characterize the liquid product of the reaction.

2. A simple experiment can be carried out to further demonstrate the probable existence of the trihalogen molecules discussed in this thesis. The recombination of iodine atoms in the presence of a small amount of chlorine gas (diluted with argon) should lead to the formation of some ICl if the intermediate ICl_2 is important.

In the same experiment, the rate of

$$2ICl \rightleftharpoons I_2 + Cl_2$$

can be measured if it falls within certain rather wide limits.

3. It is proposed that kinetic flash photolysis techniques be extended to the ultraviolet region, and, in view of current interest in the rate of recombination of oxygen atoms, that reactions in the oxygen-ozone-inert gas system be studied.

4. It is further proposed that the rates of most of the reactions in Volman's mechanism (2) for the decomposition of hydrogen peroxide could be measured by ultraviolet flash photolysis.

5. Formic acid rearranges on illumination to give hydrogen and carbon dioxide, or alternatively water and carbon monoxide (3). It is said that both processes are intramolecular. This conclusion could be easily verified (or denied) by means of some simple experiments with formic acid variously labelled with deuterium and O^{18}.

6. The infrared emission measurements under way in this laboratory furnish one example of an investigation in which the time response of an electronic detector is slow enough to interfere with interpretation of the experimental results. A general method of data reduction for such cases is proposed:

The observed signal is to be expressed as a power series in time, $\sum a_n t^n$. A similar series $\sum b_n t^n$ represents the "true" signal, corrected for the distortion introduced by the detector. A particular detector is characterized by a unique and usually very simple relation between the a's and b's. For the case of a photoconductive cell which can be represented as possessing an RC time constant γ, the

relation is

$$b_n = a_n + (n+1)\gamma a_{n+1} .$$

7. In the study of reduction reactions initiated by electrons in liquid ammonia, rate data would sometimes be of interest. For example, the question (4,5) of whether aluminum exists in the +1 valence state in liquid ammonia could be settled by a spectrophotometric measurement of the rate of disappearance of electrons from a solution of aluminum (III) iodide and potassium.

It would also be instructive to attempt to carry out the above rate measurement, or a similar one, coulometrically.

8. An investigation of the decomposition of NO_3F in the shock tube is suggested.

9. Octahedral trichelate complexes of transition metal ions racemize either by intramolecular rearrangement or by dissociation. In the second case the observation that the rates of dissociation and racemization coincide does not elucidate the mechanism of the process; removal of one ligand does not remove the asymmetry of the ion.

Exchange experiments with labelled bipyridine or phenanthroline are proposed as a check on the work of Davies and Dwyer (6) and Basolo et al. (7) and as a means

of obtaining further information about the dissociative racemization. The observed rate (8) of exchange of $Fe^{55}(II)$ with $Fe(II)(bipy)_3$ and $Fe(II)(phenan)_3$ is not very consistent with the results of the above authors.

REFERENCES FOR PROPOSITIONS

1. H. Burwasser and H. A. Taylor, J. Chem. Phys. 23, 2295 (1955).

2. D. H. Volman, J. Chem. Phys. 17, 947 (1949).

3. M. Burton, J. Am. Chem. Soc. 58, 1655 (1936).

4. G. W. Watt and J. H. Braun, J. Am. Chem. Soc. 78, 5494 (1956).

5. W. L. Taylor, E. Griswold and J. Kleinberg, J. Am. Chem. Soc. 77, 294 (1955).

6. N. R. Davies and F. P. Dwyer, Trans. Faraday Soc. 50, 1325 (1954).

7. F. Basolo, J. C. Hayes and H. M. Neumann, J. Am. Chem. Soc. 76, 3807 (1954).

8. I. B. Whitney, G. K. Schweitzer, and C. L. Comar, J. Am. Chem. Soc. 77, 1390 (1955).